

# Machine-Learning Tools for Curvature Computation in the Level-Set Method

---

Luis Ángel Larios Cárdenas

Advisor

Prof. Frédéric Gibou

# Outline

- Fundamentals
  - The level-set method.
- Curvature estimation
  - Importance.
  - Numerical improvements.
  - Preliminary machine learning research.
- Error-modeling schemes
  - Error-correcting neural networks.
- Future work

# Fundamentals

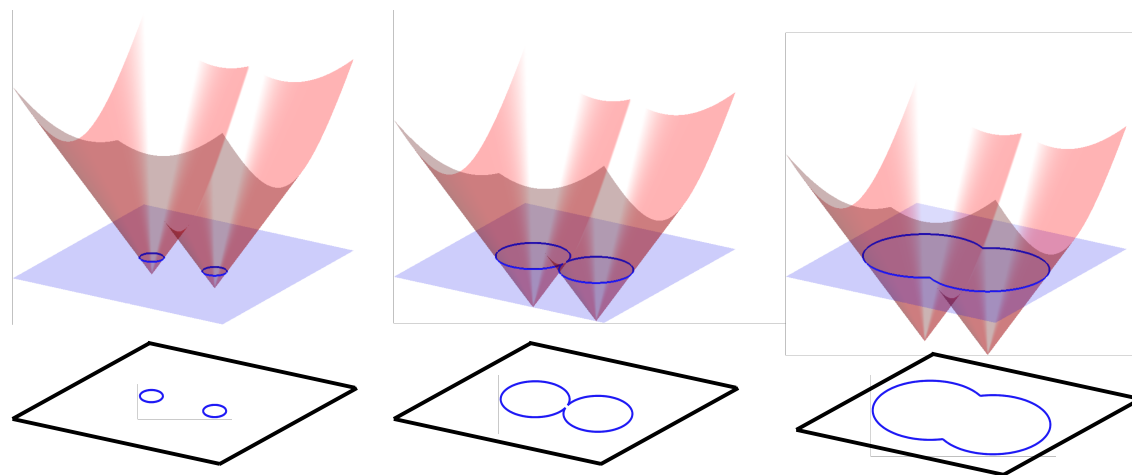
# Fundamentals

- The **level-set method (LSM)** is an implicit formulation for advecting an interface,  $\Gamma$ , captured as the **zero isocontour** of the **level-set (LS) function**,  $\phi(\mathbf{x}): \mathbb{R}^n \rightarrow \mathbb{R}$ , [Osher and Sethian 88] [Osher and Fedkiw 02][Gibou *et al.* 18].
- $\phi(\mathbf{x})$  is usually the signed normal distance function to the interface  $\Gamma$ :

$$\phi(\mathbf{x}) = \begin{cases} -d, & \mathbf{x} \in \Omega^-, \\ +d, & \mathbf{x} \in \Omega^+, \\ 0, & \mathbf{x} \in \Gamma. \end{cases}$$

- If  $\mathbf{v}(\mathbf{x})$  is a velocity field defined for all  $\mathbf{x} \in \Omega$ , the evolution of  $\phi(\mathbf{x})$  satisfies the Hamilton-Jacobi **level-set equation**:

$$\phi_t + \mathbf{v} \cdot \nabla \phi = 0$$



LS representation of a free boundary in 2D  
(Courtesy of [Gibou *et al.* 18]).

# Fundamentals

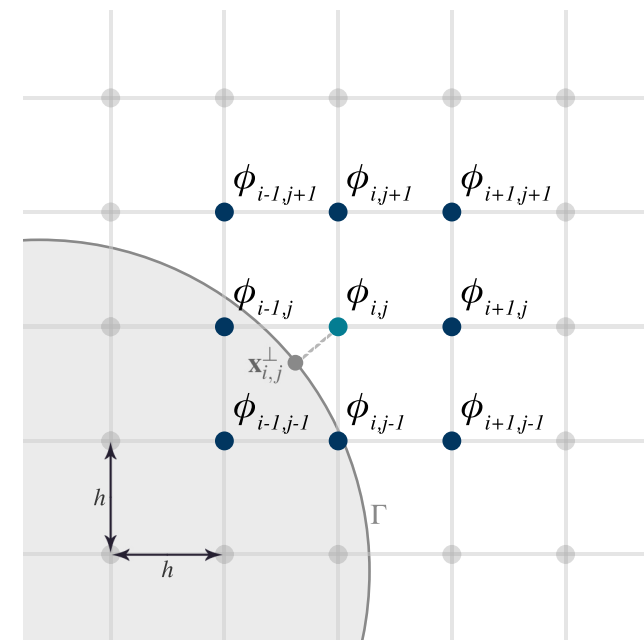
- It is straightforward to compute normal vectors and mean curvature [Min and Gibou 07][Du Ch  n   et al. 08]:

$$\hat{\mathbf{n}} = \frac{\nabla\phi}{\|\nabla\phi\|}, \quad \kappa = \nabla \cdot \frac{\nabla\phi}{\|\nabla\phi\|}$$

- To maintain the signed-distance property, we **reinitialize**  $\phi(\mathbf{x})$  periodically by solving the **reinitialization equation** [Sussman et al. 94] to steady state (or up to  $\nu$  iterations):

$$\phi_\tau + S(\phi^0)(\|\nabla\phi\| - 1) = 0$$

- Keeping  $\phi(\mathbf{x})$  as a signed distance function is important because:
  - $\|\nabla\phi\| = 1$  simplifies computations and helps maintain the physical thickness of  $\Gamma$  in multiphase flow simulations [Salih and Ghosh 13],
  - Removes noisy features that might get amplified when computing  $\partial\phi/\partial x_i$ , and
  - Removes unstructured patterns that affect the performance and training of deep learning models [LaLC and Gibou 21a & 21b].



Stencil of vertices and level-set values used in the numerical computation of curvature at node  $(i, j)$  next to  $\Gamma$ .

# Curvature Estimation

# Why Is Curvature Important?

- Curvature is a fundamental attribute in FBP for its relation to **surface tension**,  $\mathbf{f}_\sigma$ , in physics and its **regularization property** in optimization.

*Navier-Stokes equations for incompressible flow*

$$\begin{aligned}\partial_t \rho + \mathbf{u} \cdot \nabla \rho &= 0 \\ \rho(\partial_t \mathbf{u} + \mathbf{u} \cdot \nabla \mathbf{u}) &= \nabla \cdot [\mu(\nabla \mathbf{u} + \nabla^T \mathbf{u})] - \nabla p + \mathbf{f}_\sigma \\ \nabla \cdot \mathbf{u} &= 0\end{aligned}$$

Setting  $\mathbf{u} = 0$

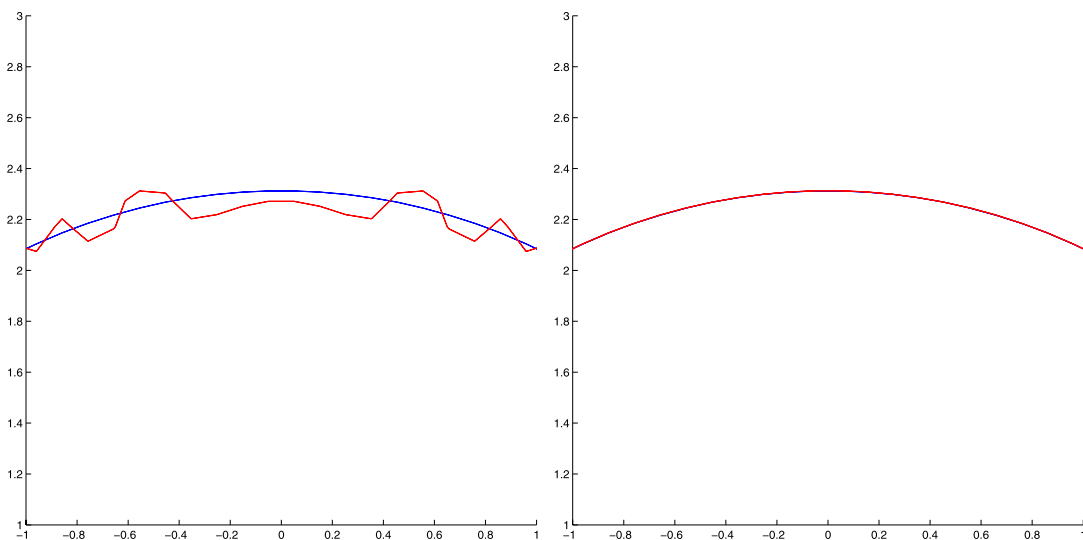
*Equilibrium condition*

$$\begin{aligned}-\nabla p + \sigma \kappa \mathbf{n} \delta_s &= 0, \\ \text{which is verified for} \\ [p] &= \sigma \kappa, \quad \kappa = \text{constant}\end{aligned}$$

- It is critical to approximate curvature accurately **at** the interface ( $\phi = 0$ )
  - To recover the continuous equilibrium solution [Popinet 18], and
  - To avoid erroneous pressure jumps,  $[p]$ , that affect breakup and coalescence [Lervåg 14].
- Computing  $\kappa$  accurately in LSM becomes challenging
  - When  $\phi(\mathbf{x})$  develops kinks close to  $\Gamma$ , or
  - Along steep portions in poorly resolved regions.

# Accurate Numerical Curvature Computation

- To compute the second-order accurate derivatives used for curvature,  $\phi(\mathbf{x})$  must be guaranteed to have some **smoothness** [Du Chéné et al. 08][Popinet 18].
- Reinitialization recovers the signed distance property and smooths out  $\phi(\mathbf{x})$  for downstream calculations.
  - We must consider  $\Gamma$ 's location and the fact that **information propagates along the characteristics**, in  $\Gamma$ 's normal direction.

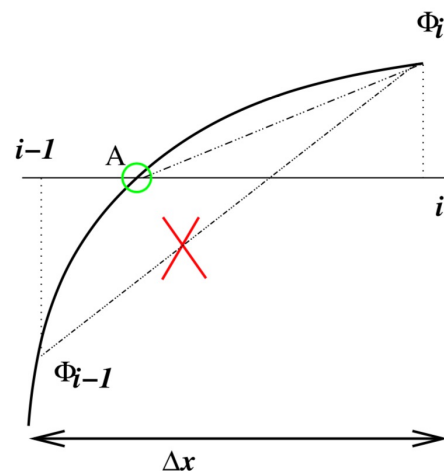


## Standard schemes

Approximating  $D^\pm$  with (W)ENO schemes from [Jiang and Peng 00].

## Fixed schemes

Sub-cell correction of [Russo and Smereka 00].



Using  $\Gamma$ 's location (A) explicitly in the approximation of one-sided derivatives (Courtesy of [Du Chéné et al. 08]).

**Second-order accurate** reinitialized LS functions [Russo and Smereka 00]:

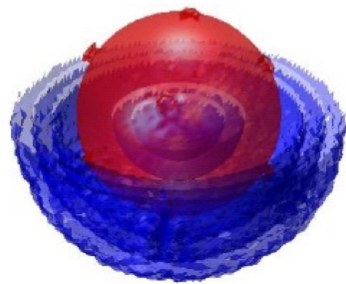
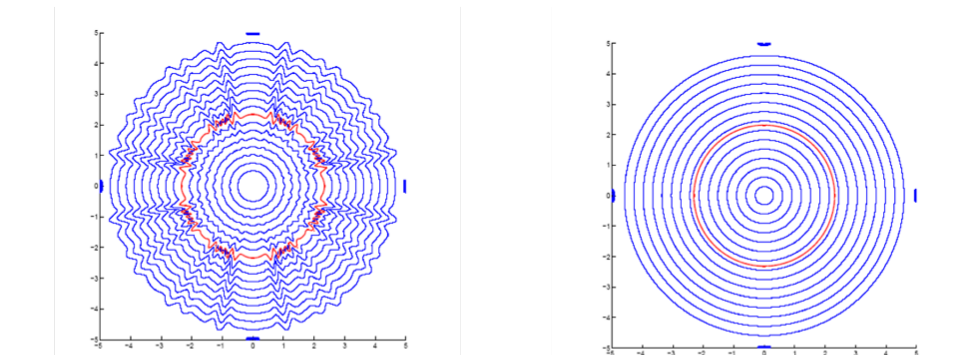
$$D_x^+ \phi_0^n = \frac{0 - \phi_0^n}{s_1} - \frac{s_1}{2} \text{minmod}(D_{xx}^0 \phi_0^n, D_{xx}^0 \phi_2^n)$$

$$\begin{array}{ccccccc} & \bullet & & \bullet & & \bullet & \\ & s_1 & & s_2 & & & \\ v_1 & & v_0 & & v_2 & & \end{array}$$

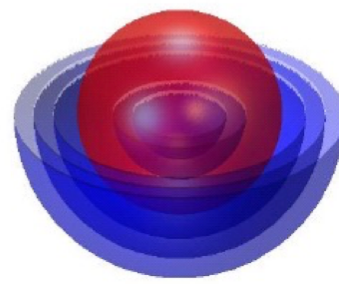
# Accurate Numerical Curvature Computation

- Reinitialization affects not **only mass preservation** but also **curvature accuracy**.

Curvature isosurfaces in 2 and 3 dimensions.



Standard schemes of  
[Jiang and Peng 00].

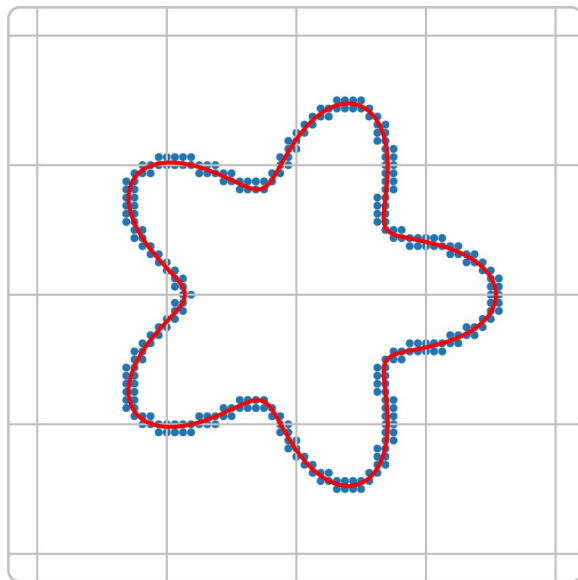


Fourth-order accurate  
reinitialization of  
[Du Chéné et al. 08].

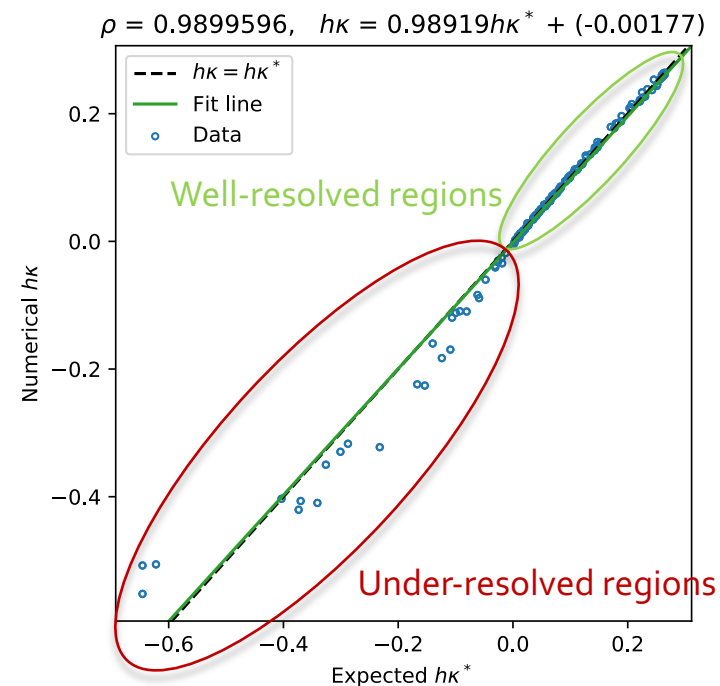
- Even second-order accurate reinitialization is prone to producing noisy curvature values.
- For this reason, [Du Chéné et al. 08] extended [Russo and Smereka 00]'s idea and designed **fourth-order accurate reinitialization schemes** and obtained **second-order accurate mean curvature**.

# Standing Challenges in Curvature Computation

- Despite these advancements:
  - Poorly resolved regions make it difficult to estimate large curvature values.
  - It may be difficult/expensive to build higher-order WENO schemes for numerical approximation in adaptive grids.



Under-resolved, concave interface regions in an irregular interface



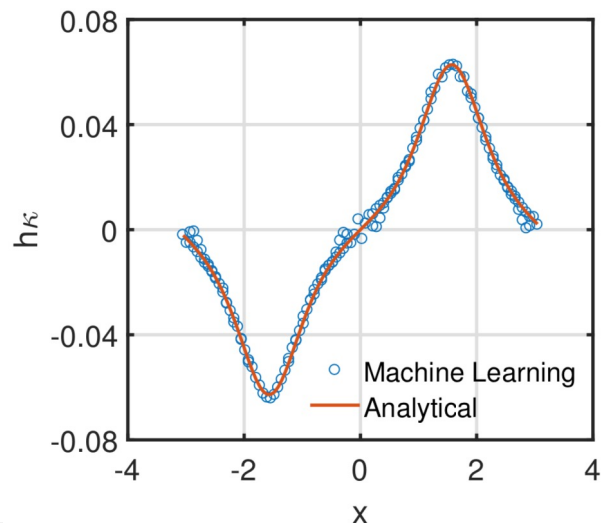
Dimensionless curvature bilinearly interpolated at the interface.

# Preliminary Research: A Neural-Network-only Approach to Estimate $\kappa$

- Inspired by the neural network (NN) of [Qi et al. 19] to estimate  $h\kappa$  in VOF:

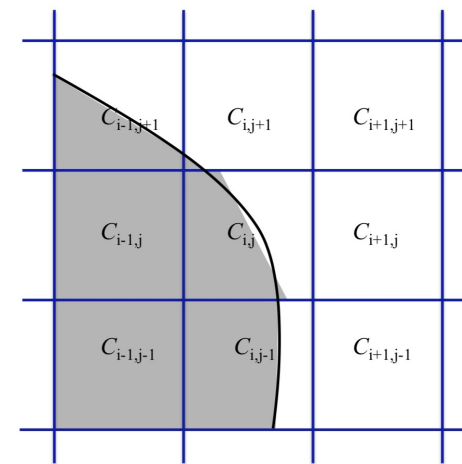
$$h\kappa_{i,j} \approx f_{VOF} \left( \begin{bmatrix} C_{i-1,j+1} & C_{i,j+1} & C_{i+1,j+1} \\ C_{i-1,j} & C_{i,j} & C_{i+1,j} \\ C_{i-1,j-1} & C_{i,j-1} & C_{i+1,j-1} \end{bmatrix} \right)$$

- Trained a *two-layered model* on samples from **circles of varying sizes**.
- Tested  $f_{VOF}(\cdot)$  on a static sine curve and in a surface-tension-driven oscillating-drop simulation with *reasonably good results*.

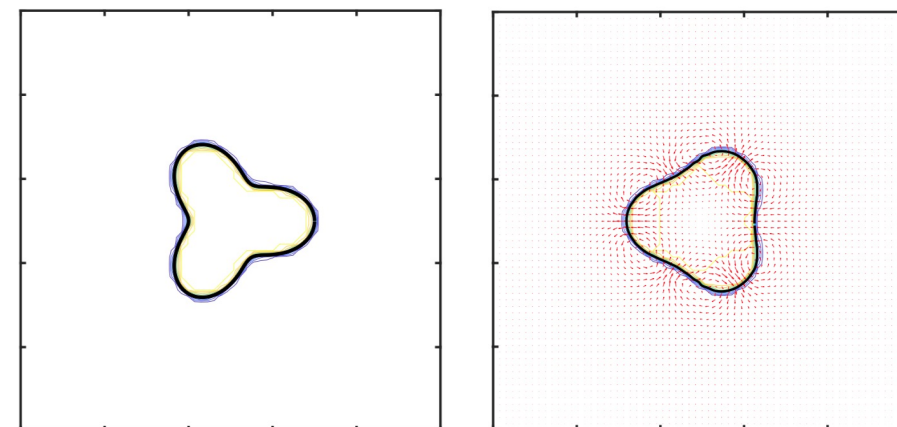


Flow simulation: initial conditions and state at  $t = 0.02$ .

Comparing exact versus ML curvature estimation for a sinusoidal curve. (All figures are courtesy of [Qi et al. 19]).



Interface cells and volume fractions constructed by the PLIC method.



# Preliminary Research: A Neural-Network-only Approach to Estimate $\kappa$

- We adapted [Qi et al. 19]'s idea to estimate  $h\kappa$  in LSM [LaLC and Gibou 21a]:

$$h\kappa_{i,j} \approx f_{LSM} \left( \begin{bmatrix} \phi_{i-1,j+1} & \phi_{i,j+1} & \phi_{i+1,j+1} \\ \phi_{i-1,j} & \phi_{i,j} & \phi_{i+1,j} \\ \phi_{i-1,j-1} & \phi_{i,j-1} & \phi_{i+1,j-1} \end{bmatrix} \right)$$

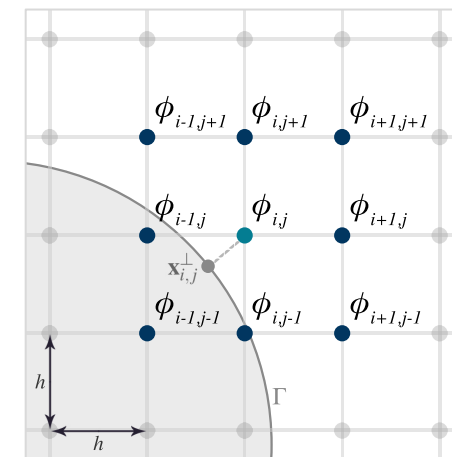
- Trained *five-layered NNs* on samples of the form  $(\phi, h\kappa^*) \in \mathbb{R}^{10}$  from **circles** with  $r \in [1.6h, 0.5 - 2h]$  uniformly spaced out with  $N_r$  values:

$$N_r(\varrho) = \left\lfloor \frac{\varrho - 8.2}{2} \right\rfloor + 1, \quad \varrho = 256, 266, 276 \quad (\leftarrow \text{nodes per unit length})$$

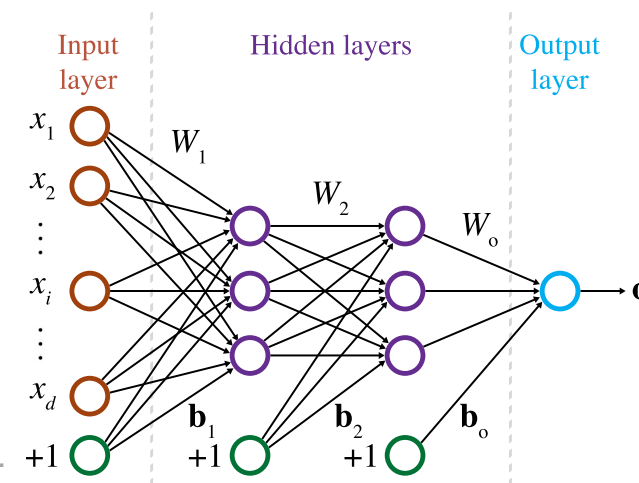
- One model per grid resolution**, optimized for **exact signed-distance** and **reinitialized** LS functions:

$$\phi_c^{sdf}(\mathbf{x}) = \|\mathbf{x} - \mathbf{x}_c\| - r, \quad \phi_c^{rls}(\mathbf{x}) = \|\mathbf{x} - \mathbf{x}_c\|^2 - r^2.$$

- Built  $\mathcal{D}$  with tuples from  $\phi_c^{rls}(\mathbf{x})$  with  $\nu = 5, 10, 15, 20$  redistancing steps.
- Randomized  $\mathbf{x}_c$  five times for each  $r$ .
- Used our parallel adaptive LSM implementation [Min and Gibou 07][Mirzadeh et al. 16].
- Split  $\mathcal{D}$  into *training* (70%), *testing* (15%), and *validation* (15%) subsets.



Nine-point-stencil LS values and  $\mathbf{x}_{i,j}^\perp$ , where  $h\kappa_{i,j}$  is computed.



Example three-layered NN.

# Preliminary Research: A Neural-Network-only Approach to Estimate $\kappa$

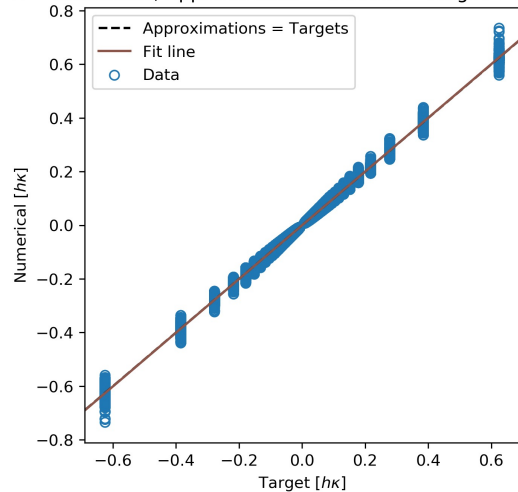
- We used **TensorFlow** and **Keras** to design and train our simple multilayer perceptrons (MLPs) with
  - Z-scores** to normalize  $\phi$  with SciKit-Learn's **StandardScaler** class.
  - 140 ReLU** neurons in each hidden layer for  $h = 1/265$ .
  - MSE** loss function for optimization.
  - Adam** optimizer with a learning rate of 0.00015.
  - Early-stopping**, which monitored the validation **MAE** (30-epoch patience).



Standardization or z-scoring

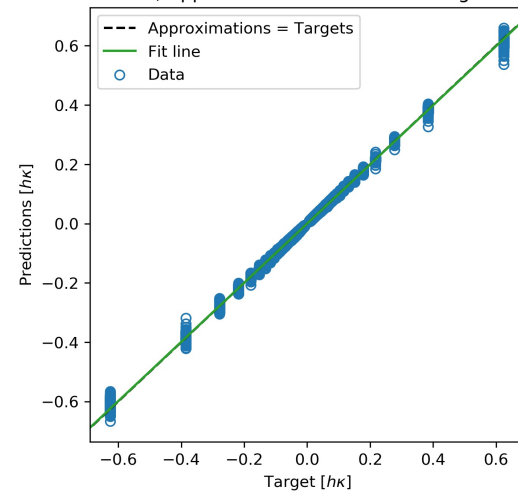
$$\psi_i \leftarrow \frac{\psi_i - \mu_\psi}{\sigma_\psi}$$

R = 0.9993089, Approximated = 1.00117 \* Target + 0.00000



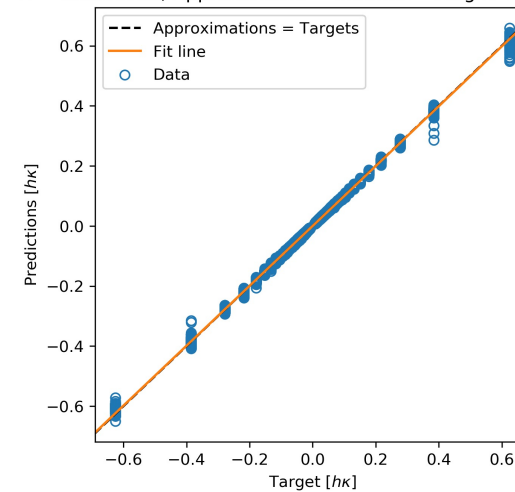
(a) Numerical method on full  $\mathcal{D}$ .

R = 0.9997432, Approximated = 0.99783 \* Target + -0.00004



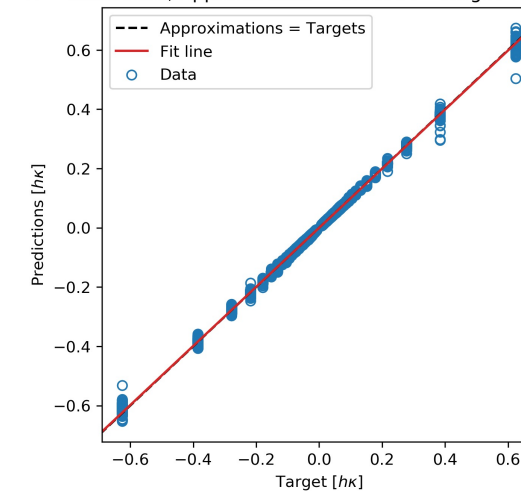
(b)  $f_{LSM}(\cdot)$  on training subset.

R = 0.9996758, Approximated = 0.99692 \* Target + -0.00005



(c)  $f_{LSM}(\cdot)$  on testing subset.

R = 0.9996696, Approximated = 0.99704 \* Target + -0.00005



(d)  $f_{LSM}(\cdot)$  on validation subset.

Fit quality for our MLP trained for  $h = 1/265$ . Agreement between numerical and neural solutions.

# Preliminary Research: A Neural-Network-only Approach to Estimate $\kappa$

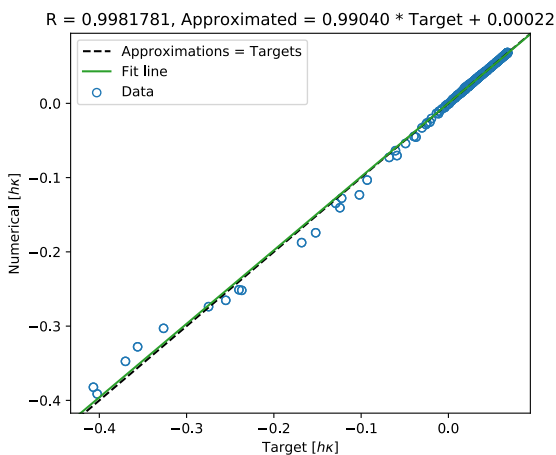
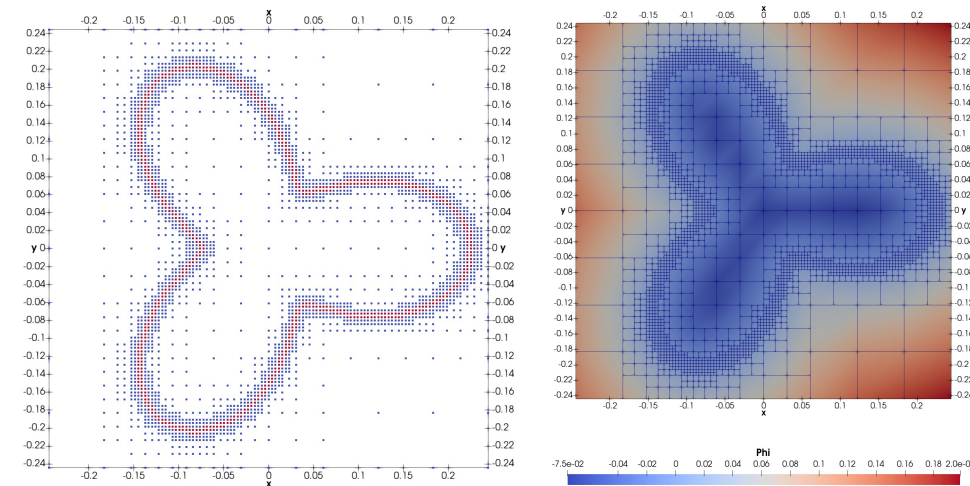
Testing  $f_{LSM}(\cdot)$  trained for  $h = 1/265$  on the *polar-rose* LS function

$$\phi_{rose}(\mathbf{x}) = \|\mathbf{x}\| - a \cos(p\theta) - b,$$

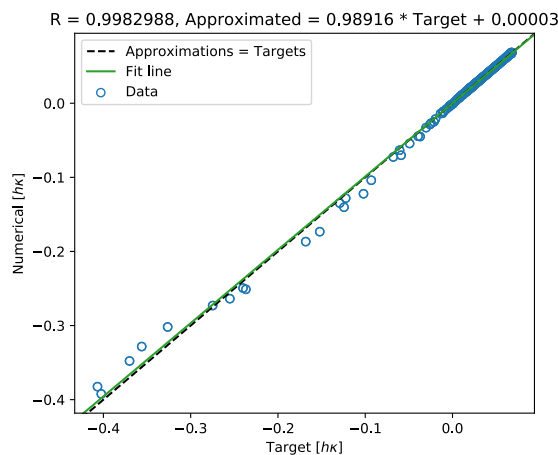
whose zero-isocontour is defined by

$$\gamma(\theta) = a \cos(p\theta) - b.$$

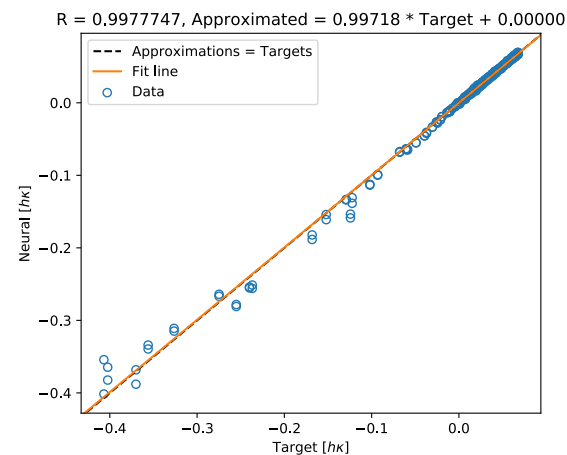
We have chosen  $p = 3$ ,  $a = 0.075$ , and  $b = 0.15$  in a domain discretized with one *quadtrees* with  $\eta = 7$  max level of refinement.



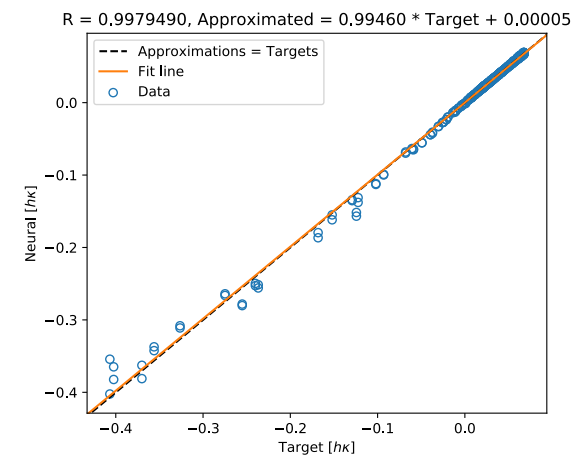
(a) Numerical at 10 iterations.



(b) Numerical at 20 iterations.



(c)  $f_{LSM}(\cdot)$  at 10 iterations.



(d)  $f_{LSM}(\cdot)$  at 20 iterations.

Fit quality for the numerical- and  $f_{LSM}(\cdot)$ -based methods.

# Preliminary Research: A Hybrid Inference System to Estimate $\kappa$

- *Can we do better than a network-only approach?*

**Yes!** By hybridization.

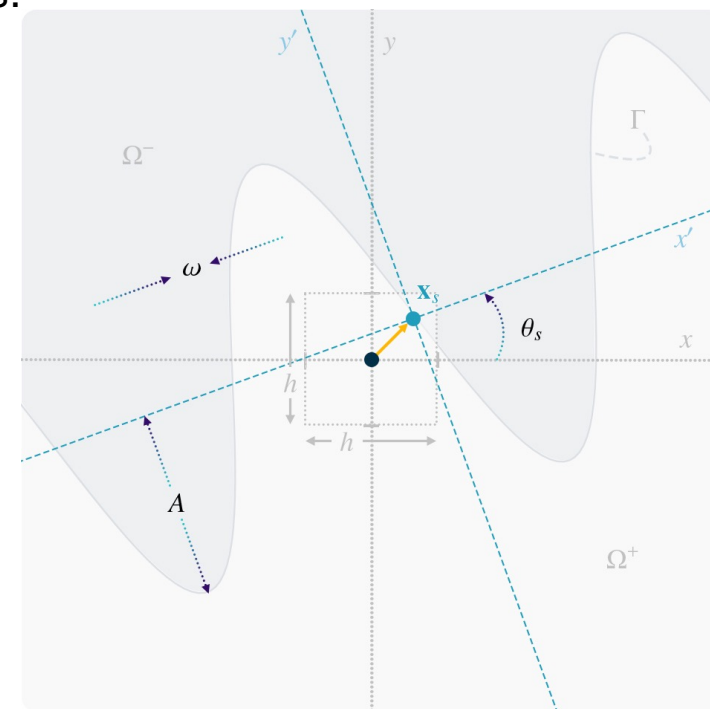
- First, we have presented **enhanced NNs** [LaLC and Gibou 21b],  $F_h(\cdot): \mathbb{R}^9 \mapsto \mathbb{R}$ , that output  $h\kappa$  for smooth two-dimensional interfaces, given a **preprocessed** nine-point stencil,  $\phi$ , of LS values.

- Added **affine-transformed sinusoidal interfaces** for training,  

$$f_s(t) = A \sin(\omega t),$$

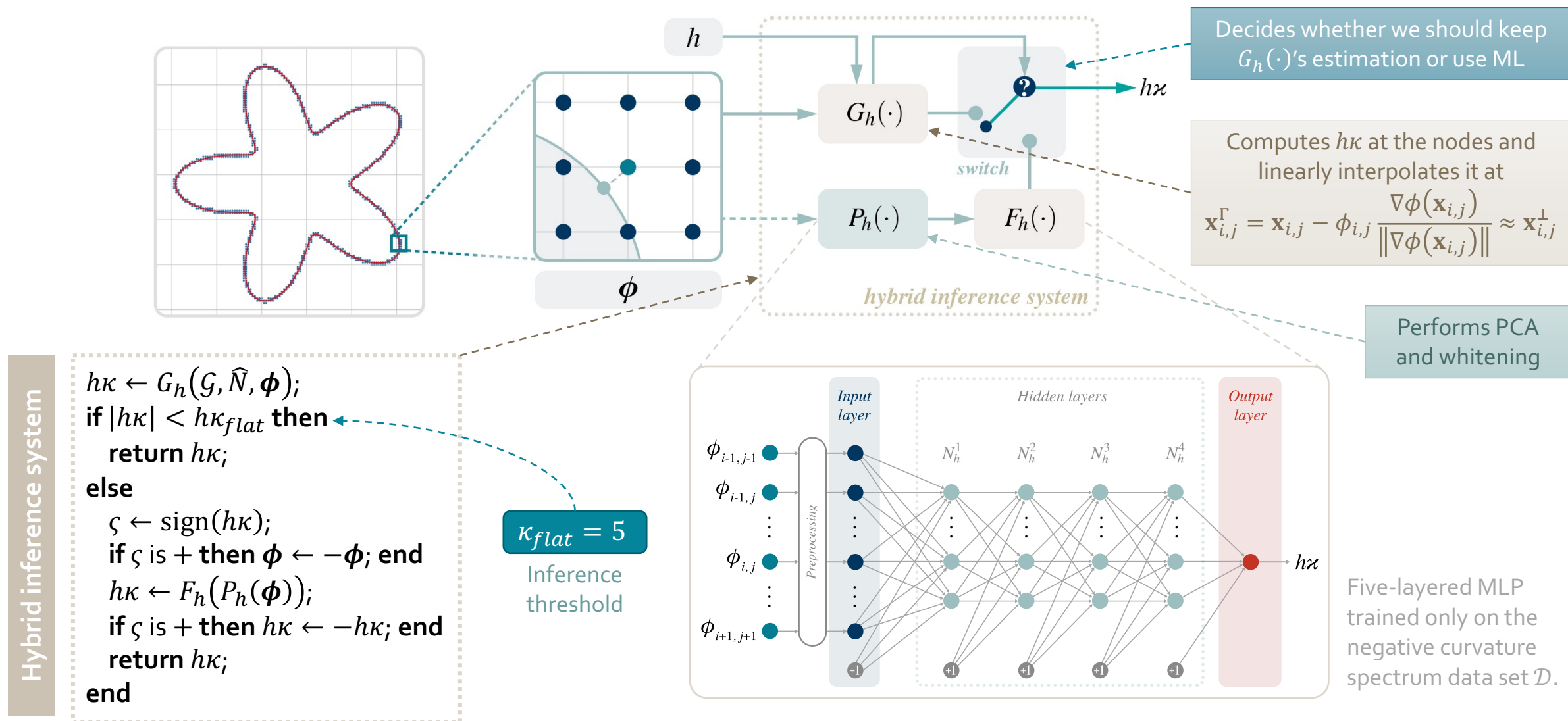
with their corresponding  $\phi_s^{sdf}(x)$  and  $\phi_s^{rls}(x)$  LS functions. Varying  $f_s(t)$  combinatorically in  $A$ ,  $\omega$ , and  $\theta_s$  with random translations ( $\mathbf{x}_s$ ).

- **Ease-off** and **histogram-based** probabilistic **subsampling**.
- **Data augmentation** by rotating stencils by  $90^\circ$  three times.
- Reduced degrees of freedom by considering only **half the curvature spectrum**. Exploited **problem's intrinsic symmetry**.
- Used  $-\kappa^* \in [0.5, 85\frac{1}{3}]$  for all grid resolutions.
- Redistributed circular interfaces uniformly on  $\kappa^*$  instead of their radii.
- Redistanced both  $\phi_s^{rls}(\mathbf{x})$  and  $\phi_c^{rls}(\mathbf{x})$  only with  $\nu = 10$  iterations.
- Preprocessed  $\phi$  with **PCA and whitening**.



Transforming  $f_s(t)$  by  $T(x_s)$  and  $R(\theta_s)$ .  
Domain partitioned into  $\Omega^-$  and  $\Omega^+$  regions.

# Preliminary Research: A Hybrid Inference System to Estimate $\kappa$



# Preliminary Research: A Hybrid Inference System to Estimate $\kappa$

- We followed the same training approach as [LaLC and Gibou 21a] except for:
  - PCA + whitening** to speed up convergence [LeCun et al. 12] using SciKit-Learn's **PCA** class.
  - 180 ReLU** neurons in each hidden layer for  $h = 1/128$  (i.e., for *unit-square quadtrees* with  $\eta = 7$  maximum level of refinement).
  - Halving the learning rate** from  $1.5 \times 10^{-4}$  to  $1.5 \times 10^{-5}$  if validation MAE does not improve for **15 epochs**.
  - Delayed **early-stopping** with a patience of 60 epochs.

Principal component analysis (PCA) is a change of basis, where the new axes are the first  $k$  singular vectors of the **covariance matrix**

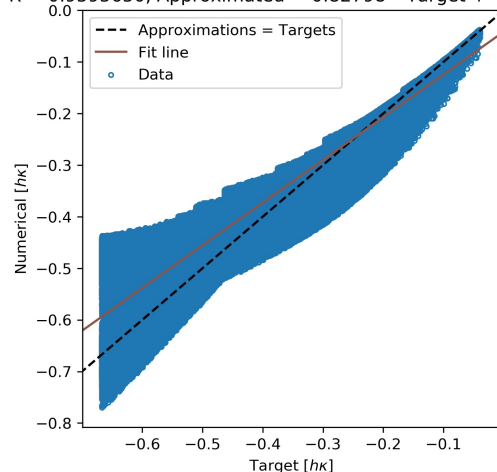
$$C = \frac{1}{n-1} (D - M)^T (D - M).$$

If  $X = D - M$  and  $C = USV^T$ , then  $X^{(k)} = XV^{(k)}$

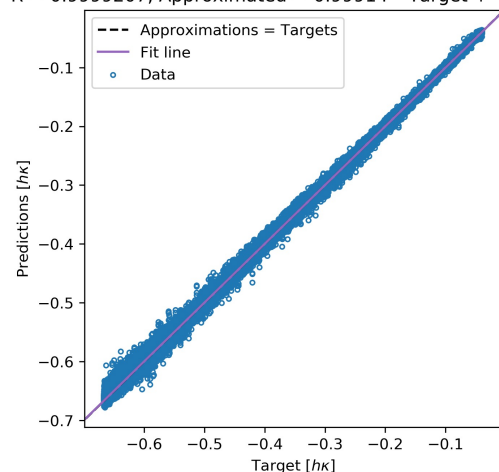
is the  $n$ -by- $k$  transformed data set, where  $V^{(k)}$  are the first  $k$  cols in  $V$ .

**Whitening:**  $X_w^{(k)} = X^{(k)}(S^{(k)})^{-\frac{1}{2}}$

R = 0.9595650, Approximated = 0.82798 \* Target + -0.04145



R = 0.9999207, Approximated = 0.99914 \* Target + -0.00024



Fit quality on  $\mathcal{D}^{rls}$  for (left)  $G_h(\cdot)$  and (right)  $F_h(\cdot)$  trained for  $\eta = 7$ .

	MAE	Max absolute error	MSE
Neural network	$1.815692 \times 10^{-1}$	7.242649	$8.291462 \times 10^{-2}$
Numerical method	4.511332	$2.926552 \times 10^1$	$5.141757 \times 10^1$

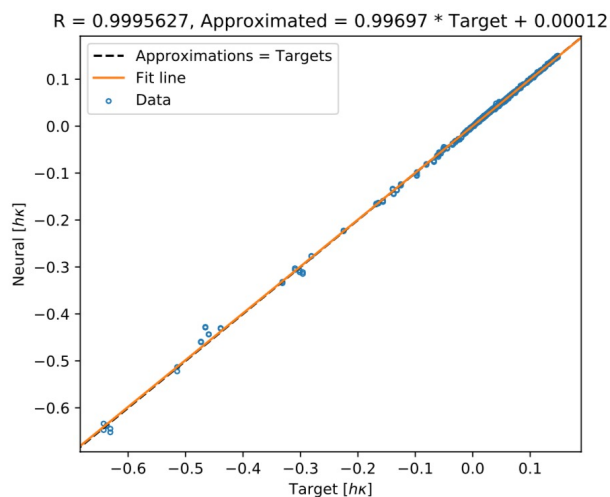
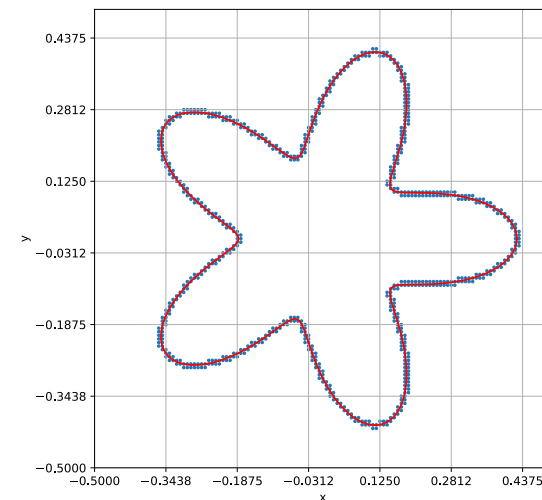
Training statistics on  $\mathcal{D}^{rls}$  in terms of  $\kappa$  for  $\eta = 7$ .

# Preliminary Research: A Hybrid Inference System to Estimate $\kappa$

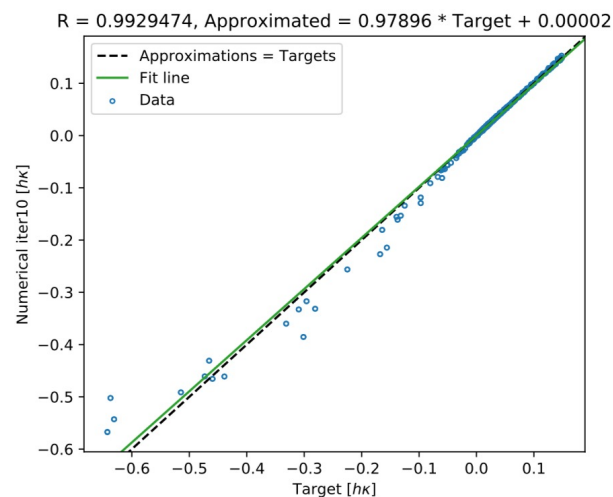
Testing our hybrid system for  $h = 2^{-7}$  on  $\phi_{\text{rose}}(\mathbf{x})$  with  $p = 5$ ,  $a = 0.12$ , and  $b = 0.305$ .

Method	Mean Absolute Error	Max Absolute Error	Mean Squared Error
Hybrid approach	$1.778957 \times 10^{-1}$	4.841265	$1.601629 \times 10^{-1}$
Numerical method, 10 iters.	$4.441347 \times 10^{-1}$	$1.726560 \times 10^1$	2.570065
Numerical method, 20 iters.	$4.046386 \times 10^{-1}$	$1.745362 \times 10^1$	2.554465

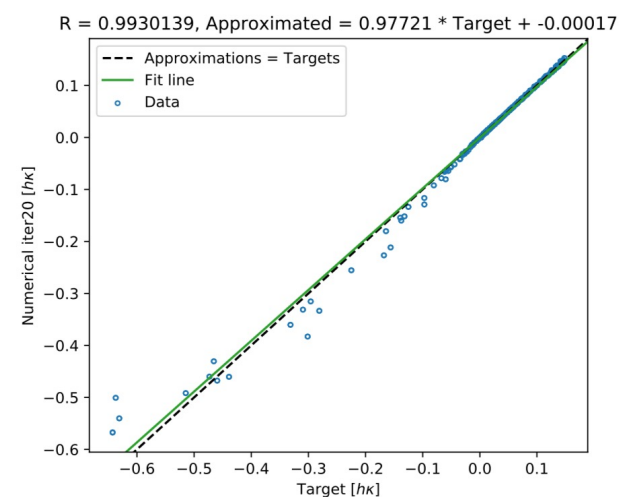
Comparing  $\kappa$  results for  $h = 1/128$  with a model with four 18o-ReLU-neuron hidden layers.



(a) Hybrid approach ( $\nu = 10$ ).



(b) Numerical  $G_h(\cdot)$  ( $\nu = 10$ ).

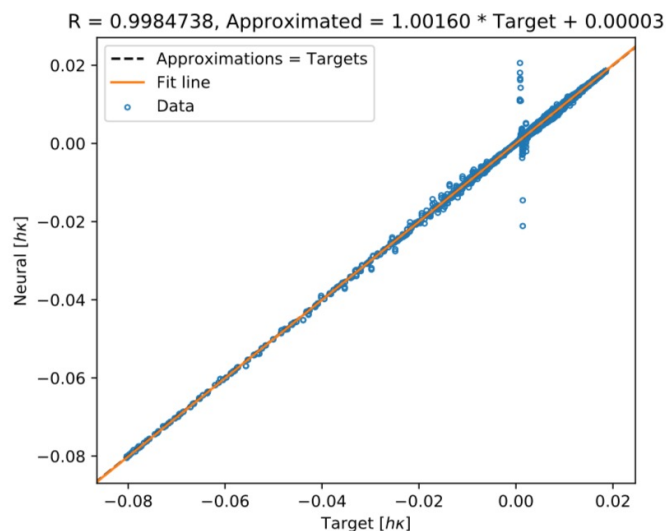


(c) Numerical  $G_h(\cdot)$  ( $\nu = 20$ ).

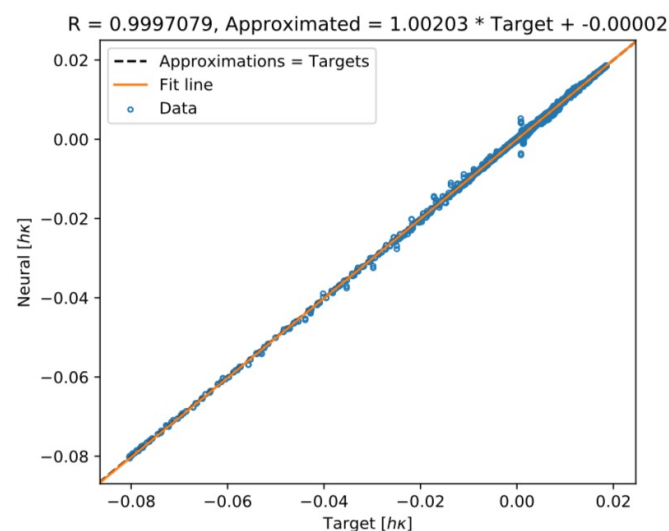
Fit quality for  $h\kappa$  using the hybrid approach and  $G_h(\cdot)$ .

# Can we do better than that?

- PCA and whitening are good for convergence but leads to **overfitting** as  $h \rightarrow 0$  (despite early stopping).
  - Can we **increase generalization**?
- The process for building  $\mathcal{D}$  and optimizing  $F_h(\cdot)$  **does not scale well** for large  $\eta$ .
  - Can we **exploit other properties** besides the problem's intrinsic symmetry?
  - Can we just **not throw away the numerical  $h\kappa$**  approximation during inference?



(a) Using PCA and whitening.



(b) Using z-scores.

Generalization of a network-only model for  $\eta = 10$  when inferring  $h\kappa$  along previous  $\phi_{rose}(\mathbf{x})$ .

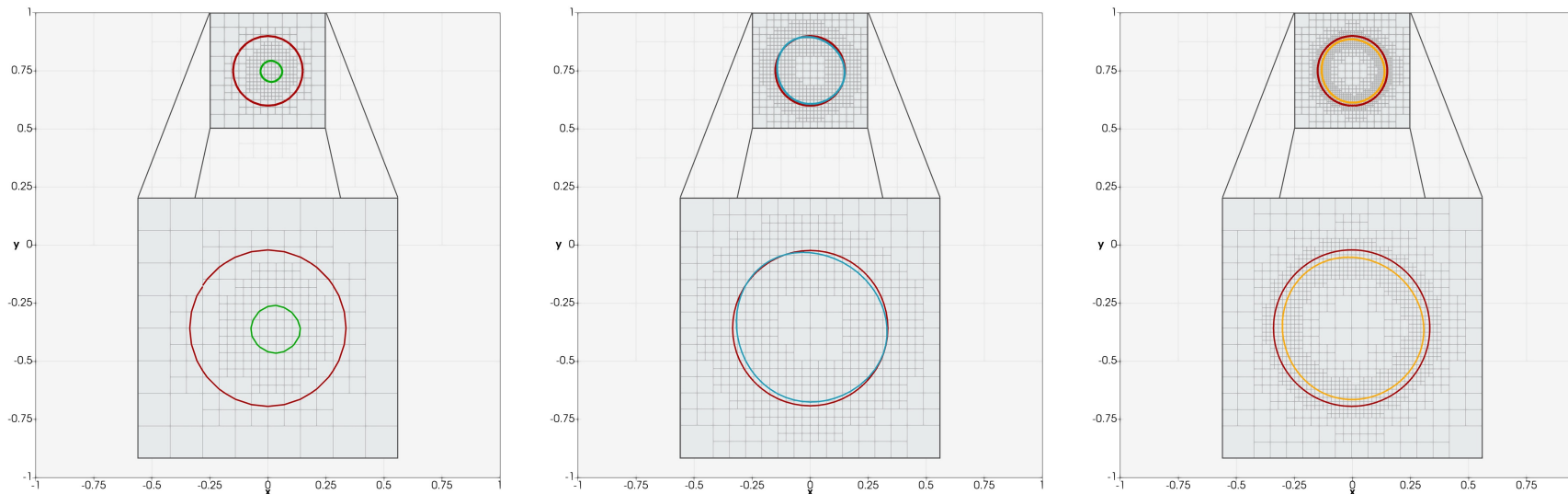
$\eta$	Approach	$ \mathcal{D} $	Params.	Units per hidden layer
7	Network-only	4'442,728	200,193	256
	Hybrid	2'330,785	99,721	180
8	Network-only	7'258,628	159,145	228
	Hybrid	3'629,297	89,081	170
9	Network-only	9'315,620	148,281	220
	Hybrid	5,205,788	52,521	130
10	Network-only	12'592,164	159,145	228
	Hybrid	6,273,339	31,401	100

Topological analysis. Data-set size grows too much as  $\eta$  increases.

# Error neural modeling schemes

# Introducing Error-Correcting Neural Networks (ECNets)

- Drawing inspiration from ML-augmented scalar advection [Pathak et al. 20], ECNets for semi-Lagrangian transport [LaLC and Gibou 21c] using quadtrees [Strain 99], and image-super resolution technologies [Dong et al. 14].
  - **Goal:** To compute on-the-fly corrections to a coarse grid trajectory, so that it follows that of a much finer grid.
- In [LaLC and Gibou 21c], we introduced the `MLSemiLagrangian()` routine: a hybrid advection solver for FBP.
  - `MLSemiLagrangian()` couples numerical advection with the ECNet  $\mathcal{F}_{c,f}(\cdot)$  to improve LS accuracy next to  $\Gamma^n$ .
  - Exploited advection and curvature **symmetry invariance**.



Zero-contours at the end of the 15<sup>th</sup> revolution. Left and right: numerical baseline for  $h = 2^{-6}$  and  $h = 2^{-7}$ . Center: `MLSemiLagrangian()` solution for  $h = 2^{-6}$ . Analytical disk appears in red.

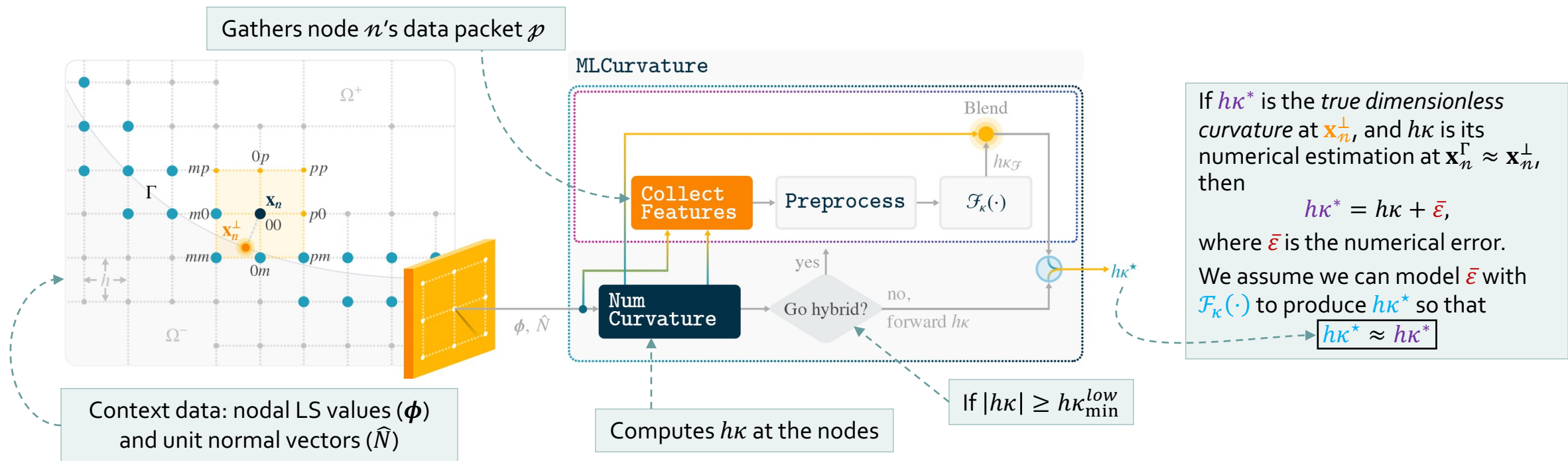
**Use case:** Rotating disk of radius 0.15, initially placed at  $(0, 0.75)$ , subject to

$$\mathbf{u}(x, y) = \frac{1}{\sqrt{2}} \begin{bmatrix} -y \\ x \end{bmatrix}$$

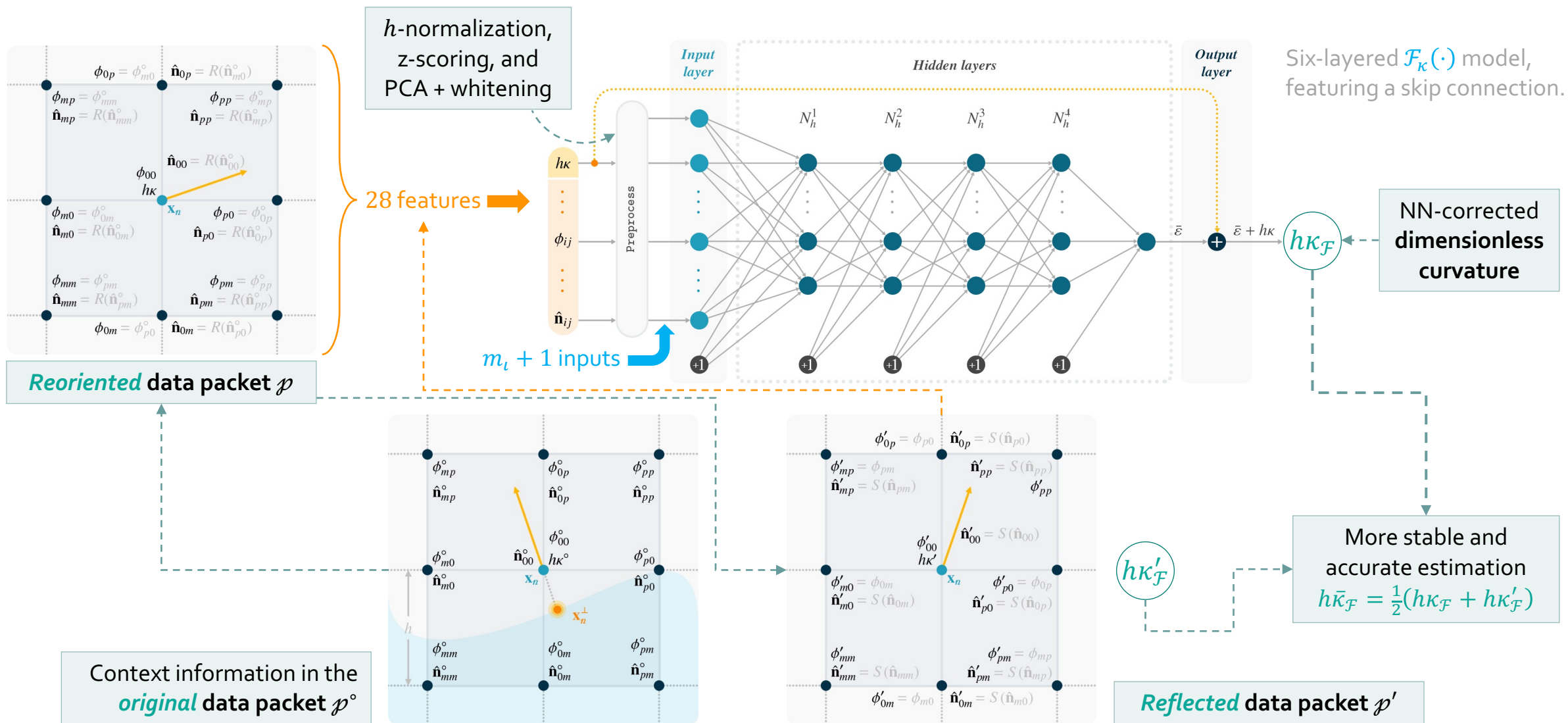
within  $\Omega \equiv [-1, +1]^2$ .

# Novel Error-Correcting Neural Network for 2D Curvature Computation

- We have proposed an `MLCurvature()` hybrid routine in [LaLC and Gibou 22] that uses an ECNet to correct the numerical error in  $h\kappa$  by:
  - Leveraging **context information** like  $\phi$  values, gradient, and  $h\kappa$  itself.
  - Enabling  $\mathcal{F}_\kappa(\cdot)$  prediction only when necessary (and its output with  $h\kappa$  near flat regions).
  - Exploiting  $\kappa$  **rotation/reflection invariance** to simplify the problem and improve stability through **double predicting**.
  - Incorporating **dimensionality reduction**, **well-balanced** data sets, and **regularization** to increase generalization.



# Novel Error-Correcting Neural Network for 2D Curvature Computation



# Novel Error-Correcting Neural Network for 2D Curvature Computation

**Algorithm 1:**  $h\kappa^* \leftarrow \text{MLCurvature}(n, \mathcal{F}_\kappa(\cdot), \phi, \hat{N}, h, h\kappa_{\min}^{\text{low}}, h\kappa_{\min}^{\text{up}})$ : Compute the dimensionless curvature for the interface node  $n$  using the standard scheme with error correction provided by  $\mathcal{F}_\kappa(\cdot)$ .

**Input:**  $n$ : node object;  $\mathcal{F}_\kappa(\cdot)$ : error-correcting neural network;  $\phi$ : nodal level-set values;  $\hat{N}$ : nodal unit normal vectors;  $h$ : mesh size;  $h\kappa_{\min}^{\text{low}}$ : minimum  $|h\kappa|$  to enable neural inference;  $h\kappa_{\min}^{\text{up}}$ :  $|h\kappa|$ 's upper bound for blending numerical with neurally corrected approximation.

**Result:**  $h\kappa^*$ : dimensionless curvature at  $\mathbf{x}_n^\Gamma$ .

```

// Numerical computation
1  $K \leftarrow \text{NumCurvature}(n.\text{stencil}, \phi, \hat{N})$ ;
2  $\mathbf{x}_n^\Gamma \leftarrow n.\mathbf{x} - \phi[n]\hat{N}[n]$ ;
3  $h\kappa \leftarrow h \cdot \text{Interpolate}(n.\text{stencil}, K, \mathbf{x}_n^\Gamma)$ ;

// Selectively enabling neural correction
4 if  $|h\kappa| \geq h\kappa_{\min}^{\text{low}}$  then
5    $p \leftarrow \text{CollectFeatures}(n.\text{stencil}, \phi, \hat{N})$ ;
6    $p.h\kappa \leftarrow h\kappa$ ;

   // Produce two samples for  $n$ 
7   transform  $p$  so that  $p.h\kappa$  is negative;
8   reorient  $p$  so that the angle of  $p.\hat{\mathbf{n}}_{00}$  lies between 0 and  $\pi/2$ ;
9    $h\kappa_{\mathcal{F}} \leftarrow \mathcal{F}_\kappa([\text{Preprocess}(p, h), p.h\kappa])$ ;
10  let  $p'$  be the reflected data packet about the line  $y = x + \beta$  going through  $n.\mathbf{x}$ ;
11   $h\kappa'_{\mathcal{F}} \leftarrow \mathcal{F}_\kappa([\text{Preprocess}(p', h), p'.h\kappa])$ ;
12   $h\bar{\kappa}_{\mathcal{F}} \leftarrow \frac{1}{2}(h\kappa_{\mathcal{F}} + h\kappa'_{\mathcal{F}})$ ;

   // Linearly blending neural and numerical estimations near zero
13  if  $|h\kappa| \leq h\kappa_{\min}^{\text{up}}$  then
14     $\lambda \leftarrow (h\kappa_{\min}^{\text{up}} - |h\kappa|) / (h\kappa_{\min}^{\text{up}} - h\kappa_{\min}^{\text{low}})$ ;
15     $h\bar{\kappa}_{\mathcal{F}} = (1 - \lambda)h\bar{\kappa}_{\mathcal{F}} + \lambda(-|h\kappa|)$ ;
16  end
17   $h\kappa^* \leftarrow \text{Sign}(h\kappa) \cdot |h\bar{\kappa}_{\mathcal{F}}|$ ;
18 else
19    $h\kappa^* \leftarrow h\kappa$ ;
20 end
21 return  $h\kappa^*$ ;

```

Computing (numerical)  $h\kappa$  at  $\mathbf{x}_n^\Gamma$

Populating  $n$ 's original data packet

Computing  $h\kappa_{\mathcal{F}}$  for  $p$

Computing  $h\kappa'_{\mathcal{F}}$  for  $p'$

Averaging into  $h\bar{\kappa}_{\mathcal{F}}$

Transitioning from  $|h\kappa|$  to  $|h\bar{\kappa}_{\mathcal{F}}|$  linearly in the range of  $[h\kappa_{\min}^{\text{low}}, h\kappa_{\min}^{\text{up}}]$

$\mathbf{p} \leftarrow \text{Preprocess}(p, h)$

$p.\phi_{ij} \leftarrow \frac{1}{h} p.\phi_{ij}$ , for  $i, j \in \{m, 0, p\}$ ;

$\mathbf{q} \leftarrow \text{Vectorize}(p)$ ;

$Q \leftarrow \text{GetStats}()$ ;

$(\boldsymbol{\mu}, \boldsymbol{\sigma}) \leftarrow Q.\text{StdScaler}$ ; // Z-scoring.

$\mathbf{z} \leftarrow (\mathbf{q} - \boldsymbol{\mu}) \oslash \boldsymbol{\sigma}$ ;

$(V^{(m_i)}, S^{(m_i)}) \leftarrow Q.\text{PCA}$ ; // Dim. reduction.

$\mathbf{p} \leftarrow (S^{(m_i)})^{-1/2} (V^{(m_i)})^T \mathbf{z}$ ;

**return**  $\mathbf{p}$ ;

We have chosen

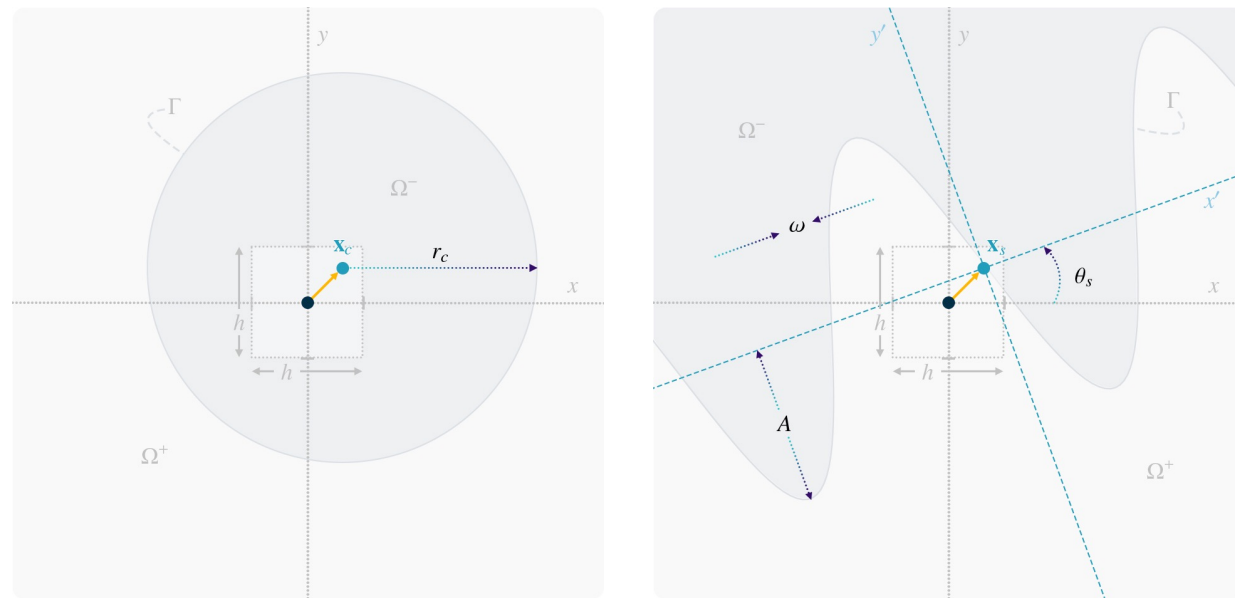
$$h\kappa_{\min}^{\text{low}} = 0.004 = h\kappa_{\min}^*$$

and

$$h\kappa_{\min}^{\text{up}} = 0.007$$

# Novel Error-Correcting Neural Network for 2D Curvature Computation

- **Data-set generation** like [LaLC and Gibou 21b], on **circular** and **sinusoidal** interfaces, except for **non-dimensional parametrization**: **Scalable across grid resolutions!**
  - Built  $\mathcal{D} = \mathcal{D}_c \cup \mathcal{D}_s$  with tuples with  $|h\kappa^*|$  between  $h\kappa_{\min}^* = \mathbf{0.004}$  and  $h\kappa_{\max}^* = \frac{2}{3}$  ( $\leftarrow$  equivalent to a circle with  $r = 1.5h$ ).
  - Data-packet **reorientation** and **reflection-based augmentation** helped **constrain** the problem and **increase**  $\mathcal{F}_\kappa(\cdot)$ 's **capacity**.
  - Not considering exact-signed-distance samples anymore, only  $\phi_c^{rls}(\mathbf{x})$  and  $\phi_s^{rls}(\mathbf{x})$  redistanced with  $\nu = 10$  iterations: **Cut down  $|\mathcal{D}|$  at least in half!**
  - Improved probabilistic subsampling in both kinds of interfaces to give each  $h\kappa^*$  "class" a fair probability of being accounted for during training.



Training interfaces and their tunable parameters in black and blue.

$\mathcal{D}_c \leftarrow \text{GenerateCircularDataSet}(\eta, h\kappa_{\min}^*, h\kappa_{\max}^*, \text{CPH}, \text{SPH2}, \nu, \text{KeepEveryX})$ 

```

1  $h \leftarrow 2^{-\eta}$ ;
2  $\kappa_{\min}^* \leftarrow h\kappa_{\min}^*/h$ ;  $\kappa_{\max}^* \leftarrow h\kappa_{\max}^*/h$ ;  $r_{\min} \leftarrow 1/\kappa_{\max}^*$ ;  $r_{\max} \leftarrow 1/\kappa_{\min}^*$ ;
3  $\text{NC} \leftarrow \lceil \text{CPH} \cdot \left( \frac{r_{\max} - r_{\min}}{h} + 1 \right) \rceil$ ;

```

Find min/max  $r$  and  $\kappa^*$  and NC for current mesh size

CPH = 2

```

4  $\bar{r} \leftarrow \frac{1}{2}(r_{\min} + r_{\max})$ ;
5  $\text{AvgSPR} \leftarrow \frac{1}{\text{KeepEveryX}} \left[ \text{SPH2} \cdot \frac{\pi}{h^2} (\bar{r}^2 - (r_{\min} - h)^2) \right]$ ;
6  $\text{SPR} \leftarrow \text{Linspace}(0.75 \cdot \text{AvgSPR}, 1.25 \cdot \text{AvgSPR}, \text{NC})$ ;

```

Use mean  $\bar{r}$  to prescribe the number of samples per  $r_c$  into SPR

SPH2 = 5  
KeepEveryX = 4

```

// Data generation loop
7  $\mathcal{D}_c \leftarrow \emptyset$ ;
8  $\text{TgtK} \leftarrow \text{Linspace}(\kappa_{\max}^*, \kappa_{\min}^*, \text{NC})$ ;
9 for  $c \leftarrow 0, 1, \dots, \text{NC} - 1$  do
10  $\kappa^* \leftarrow \text{TgtK}[c]$ ;  $r_c \leftarrow 1/\kappa^*$ ;

```

Spacing out  $\kappa^*$  from  $\kappa_{\max}^*$  to  $\kappa_{\min}^*$  into TgtK. Use this to extract  $r_c$

```

// Collect samples for radius  $r_c$  into the set  $\mathcal{S}$ 
11  $\mathcal{S} \leftarrow \emptyset$ ;

```

Gather  $r_c$  samples until  $|\mathcal{S}| \geq 2 \cdot \text{SPR}[c]$ . Use a random  $\mathbf{x}_c$  with  $r_c$  to spawn  $\phi_c(\mathbf{x})$  and discretize  $\Omega$ .

```

12 while  $|\mathcal{S}| < 2 \cdot \text{SPR}[c]$  do
13  $\mathbf{x}_c \sim \mathcal{U}(-h/2, +h/2)$ ;
14  $\phi_c(\cdot) \leftarrow \text{CircleLevelSet}(\mathbf{x}_c, r_c)$ ;
15 let  $\mathcal{B}_\Omega$  be the domain bounds ensuring that  $\|\mathbf{x} - \mathbf{x}_c\|_\infty \leq r_c + 4h$  holds for any  $\mathbf{x} \in \Omega$ ;
16  $\mathcal{G} \leftarrow \text{GenerateGrid}(\phi_c(\cdot), \eta, \mathcal{B}_\Omega, 2h\sqrt{2})$ ;

```

Evaluate  $\phi_c(\mathbf{x})$  on  $\mathcal{G}$ , reinitialize it, and compute normal vectors ( $\hat{N}$ ) and curvature ( $\kappa$ )

```

17  $\phi \leftarrow \text{Evaluate}(\mathcal{G}, \phi_c(\cdot))$ ;
18  $\phi \leftarrow \text{Reinitialize}(\phi, \nu)$ ;
19  $\hat{N} \leftarrow \text{ComputeNormals}(\mathcal{G}, \phi)$ ;
20  $\kappa \leftarrow \text{NumCurvature}(\mathcal{G}, \phi, \hat{N})$ ;
21  $\mathcal{n} \leftarrow \text{GetNodesNextToGamma}(\mathcal{G}, \phi)$ ;

```

```

22 foreach  $node\ n \in \mathcal{n}$  do
23 if  $\mathcal{U}(0, 1) \geq 1/\text{KeepEveryX}$  then skip node  $n$ ;

```

Sample each  $n$  along  $\Gamma$  with a probability of  $1/\text{KeepEveryX}$

```

24  $p \leftarrow \text{CollectFeatures}(n.\text{stencil}, \phi, \hat{N})$ ;
25  $\mathbf{x}_n^\Gamma \leftarrow n.\mathbf{x} - \phi[n]\hat{N}[n]$   $p.h\kappa \leftarrow h.\text{Interpolate}(\mathcal{G}, \kappa, \mathbf{x}_n^\Gamma)$ ;
26 let  $\xi$  be the learning tuple  $(p, h\kappa^*)$  with inputs  $p$  and expected output  $h\kappa^* := h \cdot \kappa^*$ ;
27 transform  $\xi$  so that  $p.h\kappa^*$  is negative;
28 rotate  $\xi$  so that the angle of  $p.\hat{\mathbf{n}}_{00}$  lies between 0 and  $\pi/2$ ;
29 add  $\xi$  to  $\mathcal{S}$ ;
30 let  $\xi'$  be the reflected tuple about the line  $y = x + \beta$  going through  $n.\mathbf{x}$ ;
31 add  $\xi'$  to  $\mathcal{S}$ ;

```

Tuple for  $p$

Tuple for  $p'$

```

32 end
33 end
34  $\mathcal{D}_c \leftarrow \mathcal{D}_c \cup \text{RandomSamples}(\mathcal{S}, 2 \cdot \text{SPR}[c])$ ;

```

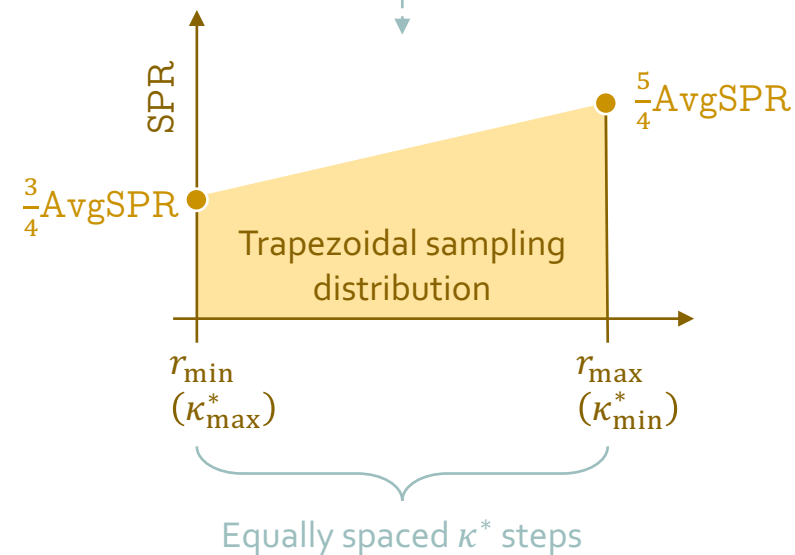
Randomly subsampling if we went over  $2 \cdot \text{SPR}[c]$

```

35 end
36 return  $\mathcal{D}_c$ ;

```

## Assembling $\mathcal{D}_c$ with circular-interface samples



$\mathcal{D}_S \leftarrow \text{GenerateSinusoidalDataSet}(\eta, h\kappa_{\min}^*, h\kappa_{\max}^*, \text{EaseOffMidMaxHKPr}, \text{NA}, \text{NT}, \nu)$ 

```

6  $\mathcal{D}_S \leftarrow \emptyset;$ 
7 foreach amplitude  $A \in \text{Linspace}(A_{\min}, A_{\max}, \text{NA})$  do
8    $\omega_{\min} \leftarrow \sqrt{h\kappa_{\max}^{\text{low}}/(h \cdot A)}$ ;  $\omega_{\max} \leftarrow \sqrt{h\kappa_{\max}^{\text{up}}/(h \cdot A)}$ ;
9    $\omega_d \leftarrow \frac{\pi}{2}(\omega_{\min}^{-1} - \omega_{\max}^{-1})$ ;
10   $\text{NF} \leftarrow \lceil \omega_d/h \rceil + 1$ ;
11  foreach frequency  $\omega \in \text{Linspace}(\omega_{\min}, \omega_{\max}, \text{NF})$  do
12     $\mathcal{S} \leftarrow \emptyset;$ 
13    foreach angle  $\theta_s \in \text{Linspace}(-\pi/2, +\pi/2, \text{NT})$ , excluding right end point do
14       $\mathbf{x}_s \sim U(-h/2, +h/2)$ ;
15       $\phi_s(\cdot) \leftarrow \text{SineLevelSet}(A, \omega, \mathbf{x}_s, \theta_s)$ ;
16      let  $\mathcal{B}_\Omega$  be the domain bounds ensuring that  $\|\mathbf{x} - \mathbf{x}_s\|_\infty \leq r_{\text{sam}} + 4h$  holds for any  $\mathbf{x} \in \Omega$ ;
17       $\mathcal{G} \leftarrow \text{GenerateGrid}(\phi_s(\cdot), \eta, \mathcal{B}_\Omega, 4h\sqrt{2})$ ;
18       $\phi \leftarrow \text{Evaluate}(\mathcal{G}, \phi_s(\cdot))$ ;
19       $\phi \leftarrow \text{Reinitialize}(\phi, \nu)$ ;
20       $\hat{N} \leftarrow \text{ComputeNormals}(\mathcal{G}, \phi)$ ;
21       $\kappa \leftarrow \text{NumCurvature}(\mathcal{G}, \phi, \hat{N})$ ;
22       $\mathcal{N} \leftarrow \text{GetNodesNextToGamma}(\mathcal{G}, \phi)$ ;
23      foreach node  $n \in \mathcal{N}$  do
24        compute the target  $h\kappa^*$  at the nearest point,  $\mathbf{x}_n^+$ , to  $n \cdot \mathbf{x}$  on the sinusoidal interface;
25        if  $\|n \cdot \mathbf{x} - \mathbf{x}_n^+\|_2^2 > r_{\text{sam}}^2$  or  $|h\kappa^*| < h\kappa_{\min}^*$  then skip node  $n$ ;
26        // Prob. sampling:  $\Pr(|h\kappa^*| \geq h\bar{\kappa}_{\max}^*) = \text{EaseOffMidMaxHKPr}$  and  $\Pr(|h\kappa^*| = h\kappa_{\min}^*) = 0.01$ 
27         $q \leftarrow \min(1, (|h\kappa^*| - h\kappa_{\min}^*) / (h\bar{\kappa}_{\max}^* - h\kappa_{\min}^*))$ ;
28        if  $U(0, 1) \leq \text{EaseOff}(0.01, \text{EaseOffMidMaxHKPr}, q)$  then
29           $p \leftarrow \text{CollectFeatures}(n.\text{stencil}, \phi, \hat{N})$ ;
30           $\mathbf{x}_n^r \leftarrow n \cdot \mathbf{x} - \phi[n]\hat{N}[n]$ ;  $p.h\kappa \leftarrow h \cdot \text{Interpolate}(\mathcal{G}, \kappa, \mathbf{x}_n^r)$ ;
31          let  $\xi$  be the learning tuple  $(p, h\kappa^*)$  with inputs  $p$  and expected output  $h\kappa^*$ ;
32          transform  $\xi$  so that  $p.h\kappa^*$  is negative;
33          rotate  $\xi$  so that the angle of  $p.\hat{\mathbf{n}}_{00}$  lies between 0 and  $\pi/2$ ;
34          add  $\xi$  to  $\mathcal{S}$ ;
35          let  $\xi'$  be the reflected tuple about the line  $y = x + \beta$  going through  $n \cdot \mathbf{x}$ ;
36          add  $\xi'$  to  $\mathcal{S}$ ;
37        end
38      end
39       $\mathcal{D}_S \leftarrow \mathcal{D}_S \cup \mathcal{S}$ ;
40    end
41 end
42 return  $\mathcal{D}_S$ ;

```

For each  $A$ , set the frequency  $\omega_{\min}$  and  $\omega_{\max}$  bounds to ensure  $|h\kappa_{\max}^*| \in [\kappa_{\max}^{\text{low}}, \kappa_{\max}^{\text{up}}]$

Dist. between the first crests at  $\omega_{\min}$  and  $\omega_{\max}$  defines # of  $\omega$  steps

// Collect samples for interface  $A\sin(\omega t)$  into  $\mathcal{S}$   
**foreach** angle  $\theta_s \in \text{Linspace}(-\pi/2, +\pi/2, \text{NT})$ , **excluding right end point** **do**

For each  $(A, \omega)$  pair, vary  $\theta_s$  and pick a random  $\mathbf{x}_s$

Evaluate  $\phi_s(\mathbf{x})$  on  $\mathcal{G}$ , reinitialize it, and compute normal vectors ( $\hat{N}$ ) and curvature ( $\kappa$ )

Only nodes inside samp. circ. or if  $|h\kappa^*| \geq h\kappa_{\min}^*$

Sample each  $n$  by following an ease-off prob. distribution

Tuple for  $p$

Tuple for  $p'$

```

1  $h \leftarrow 2^{-\eta}$ ;
2  $\kappa_{\min}^* \leftarrow h\kappa_{\min}^*/h$ ;  $\kappa_{\max}^* \leftarrow h\kappa_{\max}^*/h$ ;  $A_{\min} \leftarrow 4/\kappa_{\max}^*$ ;  $A_{\max} \leftarrow 1/\kappa_{\min}^*$ ;
3  $r_{\text{sam}} \leftarrow 2A_{\max}$ ;
4  $h\kappa_{\max}^{\text{low}} \leftarrow \frac{1}{2}h\kappa_{\max}^*$ ;  $h\kappa_{\max}^{\text{up}} \leftarrow h\kappa_{\max}^*$ ;
5  $h\bar{\kappa}_{\max}^* \leftarrow \frac{1}{2}(h\kappa_{\max}^{\text{low}} + h\kappa_{\max}^{\text{up}})$ ;

```

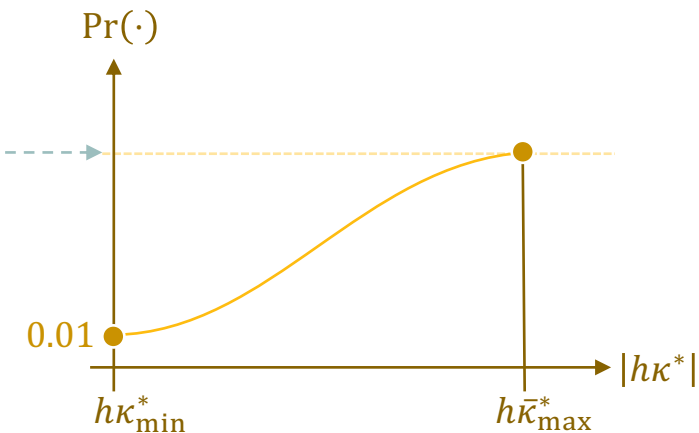
Find min/max  $\kappa^*$  and  $A$  for  $h$   
 Define sampling radius  $r_{\text{sam}}$

Set bounds  $h\kappa_{\max}^{\text{low}} \leq \max_{\Omega} |h\kappa^*| \leq h\kappa_{\max}^{\text{up}}$   
 along crests and the mean value  $h\bar{\kappa}_{\max}^*$

NA = 34

NT = 38

## Assembling $\mathcal{D}_S$ with sinusoidal-interface samples



EaseOffMidMaxHKPr = 0.4

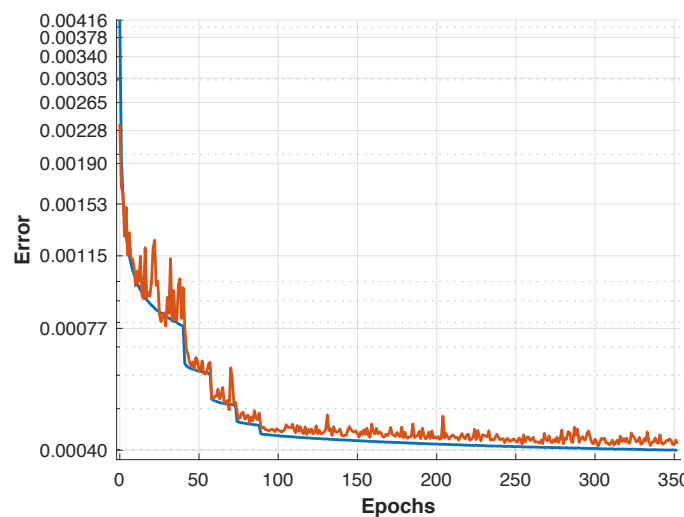
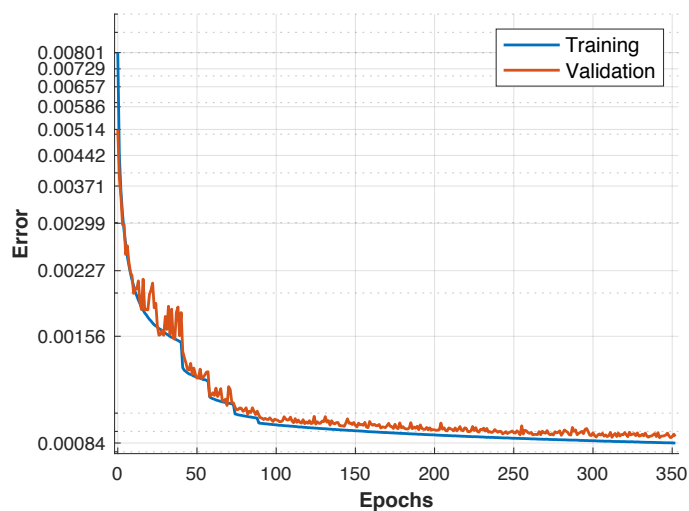
### Postprocessing histogram-based subsampling steps

1. Distribute  $\mathcal{D}_S$  into 100 bins in histogram  $\mathcal{H}$ , depending on  $h\kappa^*$ .
2. Randomly subsample overpopulated bins until  $|b| \leq \frac{2}{3} m_{\mathcal{H}}$  holds for all  $b \in \mathcal{H}$ , where  $m_{\mathcal{H}}$  is  $\mathcal{H}$ 's median.

# Novel Error-Correcting Neural Network for 2D Curvature Computation

- **Training technical details:**

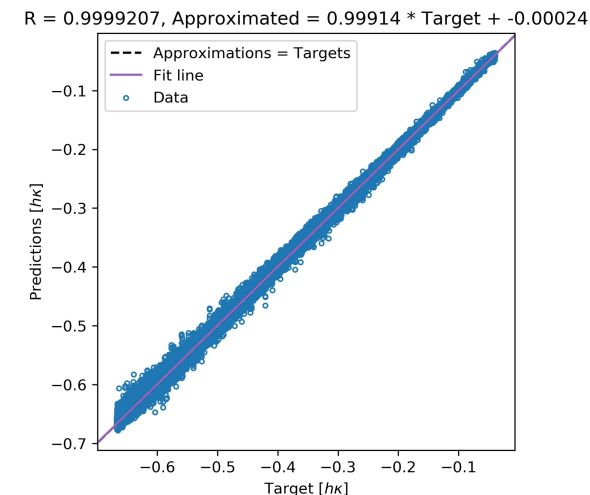
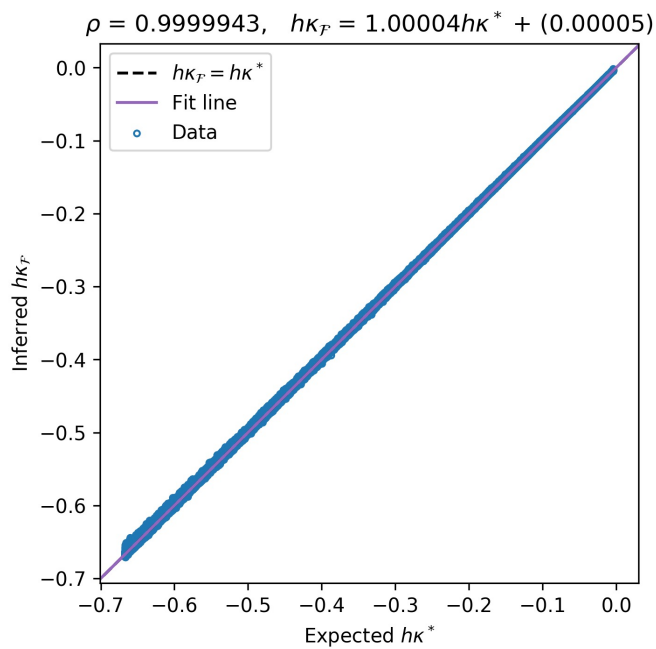
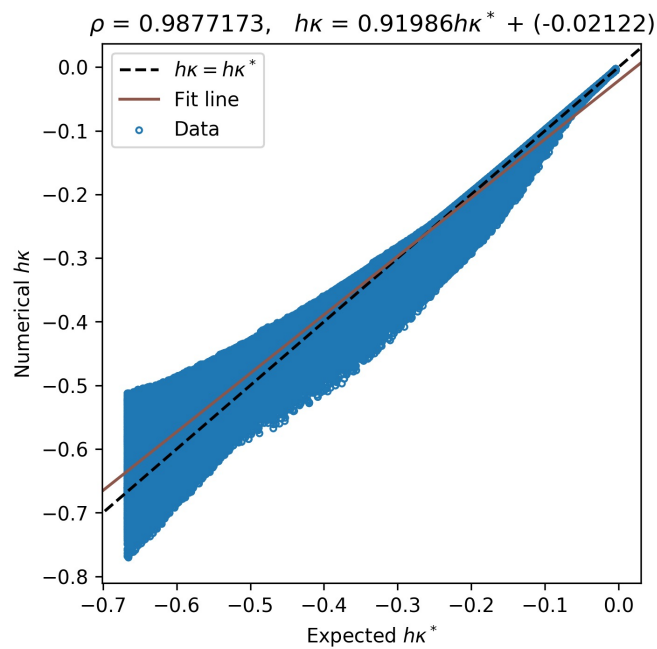
- Introduced Panda's `cut()` function to create  $100 h\kappa^*$  labels within  $\mathcal{D}$ . Then, we used these labels with SciKit-Learn's `StratifiedKFold.split()` with  $K = 10$  to split  $\mathcal{D}$  into training (70%), testing (10%), and validation (10%) subsets.
  - We discarded the remaining 10%.
  - We did not perform  $K$ -fold cross-validation for efficiency; only a couple of training instances with random weights.
- Added **L2 kernel regularization** ( $\mathcal{O}(10^{-6})$ ) in all hidden layers.
- Used **Root MSE** (RMSE), which **avored learning convergence** even more than MSE!
- Halved the learning rate from  $1.5 \times 10^{-4}$  down to  $10^{-5}$  after seeing **15 epochs** of no improvement.
- Stopped optimization after **50 epochs** of validation MAE stagnation.



Learning curves for  $\eta = 7$ .  
 Left: RMSE.  
 Right: MAE.

# Novel Error-Correcting Neural Network for 2D Curvature Computation

- Consider  $\mathcal{F}_\kappa(\cdot)$  for  $\eta = 7$  (i.e.,  $h = 1/128$ ), where
  - $N_h^i = 130$  ReLU neurons in the first four hidden layers.
  - $m_l = 18$  linear input neurons (i.e., PCA with  $m_l < 28$  components).
  - L2 =  $5 \times 10^{-6}$  kernel-regularization factor in all five hidden layers.



Fit quality on  $\mathcal{D}^{rls}$  for prior  $F_h(\cdot)$  trained for  $\eta = 7$ .

$\eta$	Method	MAE	MaxAE	RMSE
7	$\mathcal{F}_\kappa(\cdot)$	$3.923205 \times 10^{-4}$	$1.541521 \times 10^{-2}$	$6.269966 \times 10^{-4}$
	Baseline	$1.977165 \times 10^{-2}$	$1.541942 \times 10^{-1}$	$3.090897 \times 10^{-2}$

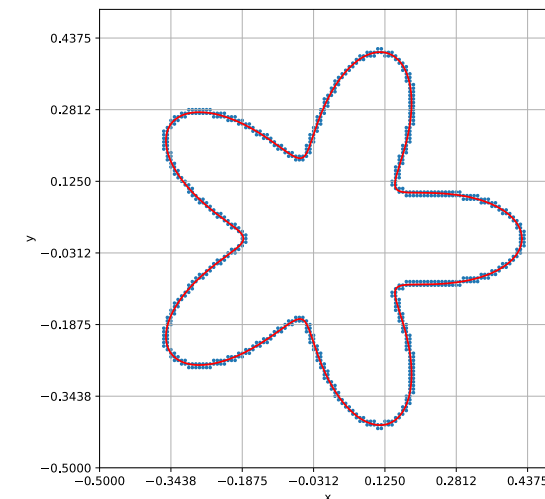
Learning  $h\kappa$  and  $h\kappa_{\mathcal{F}}$  error statistics on  $\mathcal{D}$  for  $\eta = 7$ .

Fit quality on  $\mathcal{D}$  for (left) numerical method and (right)  $\mathcal{F}_\kappa(\cdot)$  trained for  $\eta = 7$ .

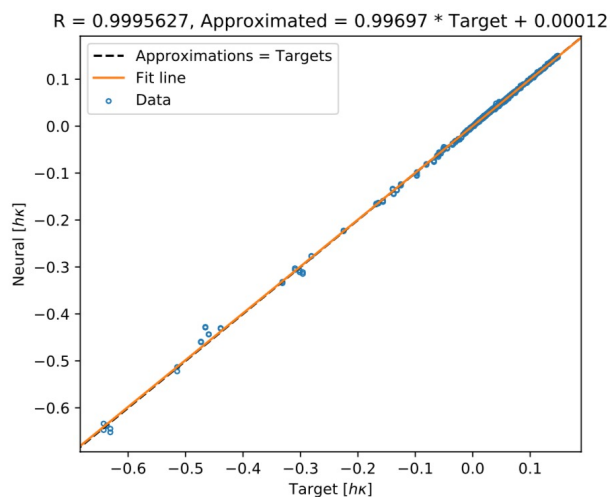
# Novel Error-Correcting Neural Network for 2D Curvature Computation

Testing `MLCurvature()` for  $h = 2^{-7}$  on  $\phi_{rose}(\mathbf{x})$  with  $p = 5$ ,  $a = 0.12$ , and  $b = 0.305$ .

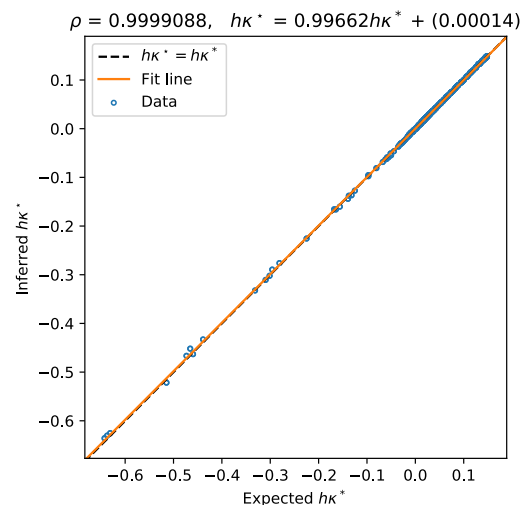
Method	MAE	Reduct. factor	MaxAE	Reduct. factor
<code>MLCurvature()</code>	$7.37148 \times 10^{-4}$	—	$1.36763 \times 10^{-2}$	—
Previous system	$1.38981 \times 10^{-3}$	1.89	$3.78224 \times 10^{-2}$	2.77
Baseline ( $\nu = 10$ )	$3.46929 \times 10^{-3}$	4.71	$1.34981 \times 10^{-1}$	9.87
Baseline ( $\nu = 20$ )	$3.16221 \times 10^{-3}$	4.29	$1.36403 \times 10^{-1}$	9.97



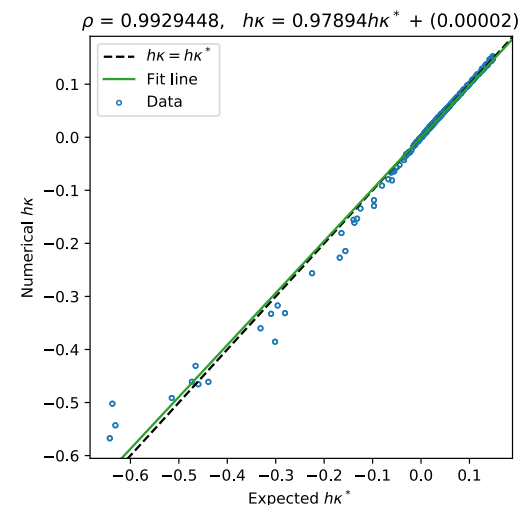
Comparing  $h\kappa$  results for  $h = 1/128$ .



(a) Old hybrid approach ( $\nu = 10$ ).



(b) `MLCurvature()` ( $\nu = 10$ ).



(c) Numerical method ( $\nu = 10$ ).

Fit quality for  $h\kappa$  and  $h\kappa^*$  using the old hybrid approach, `MLCurvature()`, and the numerical baseline.

# Novel Error-Correcting Neural Network for 2D Curvature Computation

Showing scalability to higher resolutions.

$\eta$	$m_t$	$N_h^i$	L2 factor	$ \mathcal{D} $	Parameters
6	20	130	$5 \times 10^{-6}$	1,464,020	53,951
7	18	130	$5 \times 10^{-6}$	1,473,359	53,691
8	18	120	$5 \times 10^{-6}$	1,472,775	45,961
9	18	130	$5 \times 10^{-6}$	1,464,407	53,691
10	18	130	$1 \times 10^{-5}$	1,468,513	53,691
11	18	120	$7 \times 10^{-6}$	1,462,741	45,961

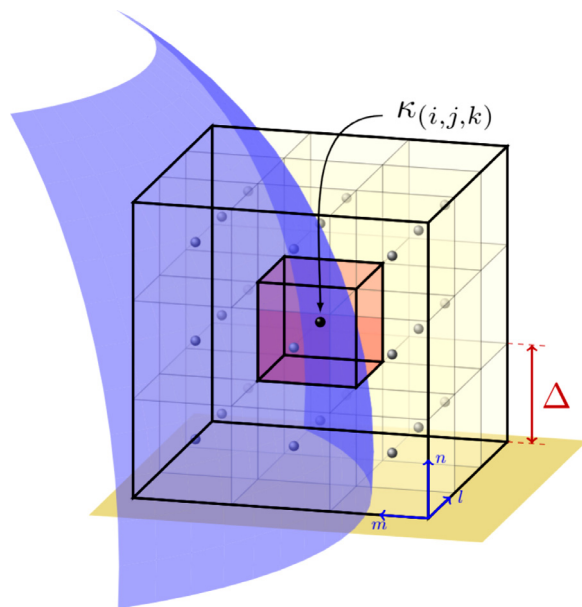
Architectural data for  $6 \leq \eta \leq 11$ .

$\eta$	Method	MAE	MaxAE	RMSE
6	$\mathcal{F}_\kappa(\cdot)$	$3.660305 \times 10^{-4}$	$1.397054 \times 10^{-2}$	$5.713122 \times 10^{-4}$
	Baseline	$1.975861 \times 10^{-2}$	$1.542492 \times 10^{-1}$	$3.095603 \times 10^{-2}$
7	$\mathcal{F}_\kappa(\cdot)$	$3.923205 \times 10^{-4}$	$1.541521 \times 10^{-2}$	$6.269966 \times 10^{-4}$
	Baseline	$1.977165 \times 10^{-2}$	$1.541942 \times 10^{-1}$	$3.090897 \times 10^{-2}$
8	$\mathcal{F}_\kappa(\cdot)$	$3.991765 \times 10^{-4}$	$1.369361 \times 10^{-2}$	$6.332734 \times 10^{-4}$
	Baseline	$1.979684 \times 10^{-2}$	$1.549115 \times 10^{-1}$	$3.094043 \times 10^{-2}$
9	$\mathcal{F}_\kappa(\cdot)$	$3.952077 \times 10^{-4}$	$1.295839 \times 10^{-2}$	$6.336660 \times 10^{-4}$
	Baseline	$1.983267 \times 10^{-2}$	$1.524857 \times 10^{-1}$	$3.097143 \times 10^{-2}$
10	$\mathcal{F}_\kappa(\cdot)$	$4.427094 \times 10^{-4}$	$1.342434 \times 10^{-2}$	$7.062269 \times 10^{-4}$
	Baseline	$1.982013 \times 10^{-2}$	$1.549863 \times 10^{-1}$	$3.095504 \times 10^{-2}$
11	$\mathcal{F}_\kappa(\cdot)$	$4.293997 \times 10^{-4}$	$1.456045 \times 10^{-2}$	$6.879887 \times 10^{-4}$
	Baseline	$1.983361 \times 10^{-2}$	$1.551221 \times 10^{-1}$	$3.098202 \times 10^{-2}$

Learning  $h\kappa$  and  $h\kappa_{\mathcal{F}}$  error statistics for  $6 \leq \eta \leq 11$ .

Networks and preprocessing objects in JSON format are available at  
[https://github.com/UCSB-CASL/Curvature\\_ECNet\\_2D](https://github.com/UCSB-CASL/Curvature_ECNet_2D)

# Ongoing and Future Work



A 27-cell stencil to compute  $\kappa_{(i,j,k)}$  in VOF  
(Courtesy of [Patel et al. 19])

- Incorporating restrictions to enforce continuity or curvature smoothness along successive interface nodes [Beucler et al. 21]?
- Adding a well-resolution classifier [Buhendwa et al. 21][Ray and Hesthaven 18] [Morgan et al. 20] instead of hand-tuning  $hk_{\min}^*$ ?
- Three-dimensional curvature computation:
  - Based on study by [Patel et al. 19] in VOF.
  - Their models were trained with well-balanced, randomized data sets of spherical patches and tested for ellipsoid, waves, and Gaussian shapes, as well as in a multiphase flow solver.
  - Experience with LSM in 2D shows that we require samples from more than just spherical interfaces.
- Per results in [Egan and Gibou 21], should we consider adding (scaled) white noise to  $\phi(\mathbf{x})$  prior to reinitialization?

**Thank You!**

# References

- [Osher and Fedkiw 02] S. Osher and R. Fedkiw. *Level Set Methods and Dynamic Implicit Surfaces*. Springer-Verlag, 2002. New York, NY.
- [Osher and Sethian 88] S. Osher and J. A. Sethian. Fronts propagating with curvature dependent speed: Algorithms based on Hamilton-Jacobi formulations. *J. Comput. Phys.*, 79(1):12–49, 1988.
- [Gibou *et al.* 18] F. Gibou, R. Fedkiw, and S. Osher. A review of level-set methods and some recent applications. *J. Comput. Phys.*, 353:82–109, 2018.
- [Sussman *et al.* 94] M. Sussman, P. Smereka, and S. Osher. A level set approach for computing solutions to incompressible two-phase flow. *J. Comput. Phys.*, 114(1):146–159, 1994.
- [Salih and Ghosh 13] A. Salih and S. Ghosh Moulic. A mass conservation scheme for level set method applied to multiphase incompressible flows. *Int. J. Comput. Meth. Eng. Sci. Mech.*, 14:271–289, 2013.
- [LaLC and Gibou 21a] L. Á. Larios-Cárdenas and F. Gibou. A deep learning approach for the computation of curvature in the level-set method. *SIAM J. Sci. Comput.*, 43(3):A1754–A1779, 2021.
- [LaLC and Gibou 21b] L. Á. Larios-Cárdenas and F. Gibou. A hybrid inference system for improved curvature estimation in the level-set method using machine learning. Submitted, <https://arxiv.org/abs/2104.02951>, 2021.
- [LaLC and Gibou 21c] L. Á. Larios-Cárdenas and F. Gibou. Error-correcting neural networks for semi-Lagrangian advection in the level-set method. Submitted, <https://arxiv.org/abs/2110.11611>, 2021.
- [LaLC and Gibou 22] L. Á. Larios-Cárdenas and F. Gibou. Error-correcting neural networks for two-dimensional curvature computation in the level-set method. Submitted, <https://arxiv.org/abs/2201.12342>, 2022.
- [Popinet 18] S. Popinet. Numerical models of surface tension. *Annu. Rev. Fluid Mech.*, 50(1):49–75, 2018.
- [Lervåg 14] K.Y. Lervåg. Calculation of interface curvature with the level-set method. <https://arxiv.org/abs/1407.7340>, 2014.
- [Jiang and Peng 00] G.-S. Jiang and D. Peng. Weighted ENO schemes for Hamilton-Jacobi equations. *SIAM J. Sci. Comput.*, 21:2126–2143, 2000.
- [Russo and Smereka 00] G. Russo and P. Smereka. A remark on computing distance functions. *J. Comput. Phys.*, 163(1): 51–67, 2000.
- [Egan and Gibou 21] R. Egan and F. Gibou. DNS Interfacial Processes. *MURI: Predicting turbulent multi-phase flows with high fidelity*. Fortnightly Meetings. March 30, 2021.

# References

- [Patel *et al.* 19] H. V. Patel, A. Panda, J. A. M. Kuipers, and E. A. J. F. Peters. Computing interface curvature from volume fractions: A machine learning approach. *Comput. Fluids*, 193:104263, 2019.
- [Ray and Hesthaven 18] D. Ray and J. S. Hesthaven. An artificial neural network as a troubled-cell indicator. *J. Comput. Phys.*, 367:166–191, 2018.
- [Morgan *et al.* 20] N. R. Morgan, S. Tokareva, X. Liu, and A. D. Morgan. A machine learning approach for detecting shocks with high-order hydrodynamic methods. *AIAA SciTech Forum*, 2020.
- [LeCun *et al.* 12] Y. A. LeCun, L. Bottou, G. B. Orr, and K.-R. Müller. *Efficient BackProp*, volume 7700 of *Lecture Notes in Comput. Sci.*, pages 9–48. Springer Berlin Heidelberg, Berlin, Heidelberg, 2012.
- [Dong *et al.* 14] C. Dong, C. C. Loy, K. He, and X. Tang. Learning a deep convolutional network for image super-resolution. In D. Fleet, T. Pajdla, B. Schiele, and T. Tuytelaars, editors, *Computer Vision – ECCV 2014*, pages 184–199, Cham, 2014. Springer International Publishing.
- [Min and Gibou 07] C. Min and F. Gibou. A second order accurate level set method on non-graded adaptive Cartesian grids. *J. Comput. Phys.*, 225(1):300–321, 2007.
- [Du Chéné *et al.* 08] A. du Chéné, C. Min, and F. Gibou. Second-order accurate computation of curvatures in a level set framework using novel high-order reinitialization schemes. *J. Sci. Comput.*, 35:114–131, 2008.
- [Mirzadeh *et al.* 16] M. Mirzadeh, A. Guittet, C. Burstedde, and F. Gibou. Parallel level-set methods on adaptive tree-based grids. *J. Comput. Phys.*, 322:345–364, 2016.
- [Pathak *et al.* 20] J. Pathak, M. Mustafa, and K. Kashinath. Using machine learning to augment coarse-grid computational fluid dynamics simulations. <https://arxiv.org/abs/2010.00072>, 2020.
- [Qi *et al.* 19] Y. Qi, J. Lu, R. Scardovelli, S. Zaleski, and G. Tryggvason. Computing curvature for volume of fluid methods using machine learning. *J. Comput. Phys.*, 377:155–161, 2019.
- [Strain 99] J. Strain. Semi-Lagrangian methods for level set equations. *J. Comput. Phys.*, 151:498–533, 1999.
- [Beucler *et al.* 21] T. Beucler, M. Pritchard, S. Rasp, J. Ott, P. Baldi, and P. Gentile. Enforcing analytic constraints in neural networks emulating physical systems. *Phys. Rev. Lett.*, 126(9):098302, 2021.
- [Buhendwa *et al.* 21] A. B. Buhendwa, D. A. Bezgin, and N. Adams. Consistent and symmetry preserving data-driven interface reconstruction for the level-set method. <https://arxiv.org/abs/2104.11578>, 2021.